IPA-1 a putative chromatin remodeler/helicase-related protein of *Trichoderma virens* plays important roles in antibiosis against *Rhizoctonia solani* and induction of *Arabidopsis* systemic disease resistance

Magnolia Estrada-Rivera[1¶], Miguel Ángel Hernández-Oñate[2¶], Mitzuko Dautt-Castro[1], José de Jesús Gallardo Negrete[1], Oscar Guillermo Rebolledo-Prudencio[1], Edith Elena Uresti-Rivera[3], Catalina Arenas-Huertero[4], Alfredo Herrera-Estrella[5]*, Sergio Casas-Flores[1]*.

[1]IPICYT, División de Biología Molecular. Camino a la presa San José No. 2055, Colonia Lomas 4a sección. C.P. 78216. San Luis Potosí, SLP., Mexico. [2]CONACYT- Centro de Investigación en Alimentación y Desarrollo, Carretera Gustavo Enrique Astiazarán Rosas No. 46, La Victoria, CP. 83304. Hermosillo, Sonora, Mexico. [3]Facultad de Ciencias Químicas, Departamento de Inmunología y Biología Celular y Molecular, Universidad Autónoma de San Luis Potosí, Av. Salvador Nava s/n, Zona Universitaria, 78290, San Luis Potosí, Mexico. [4]Facultad de Ciencias, Universidad Autónoma de San Luis Potosí, Av. Chapultepec No. 1570. Priv. del Pedregal,, 78295, San Luis Potosí, Mexico. [5]Laboratorio Nacional de Genómica para la Biodiversidad, CINVESTAV-Irapuato, C.P. 36824, Irapuato, Gto., México

*Author for correspondence:
Sergio Casas-Flores
Phone: + 1 52 444 8342046
E-mail: scasas@ipicyt.edu.mx

Fax +1 52 444 8342010

*Alfredo Herrera-Estrella

Phone: +1 52 462 1663000;

Fax +1 52 462 6245849

E-mail: alfredo.herrera@cinvestav.mx

¶**These authors contributed equally to this work.**

Abstract

Trichoderma spp. are filamentous fungi that colonize plant roots conferring beneficial effects to plants, indirectly through the induction of their defense systems or directly through the suppression of phytopathogens in the rhizosphere. Transcriptomic analyses of *Trichoderma* emerged as a powerful method for identifying the molecular events underlying the establishment of this beneficial relationship. Here, we focus on the transcriptomic response of *Trichoderma virens* during its interaction with *Arabidopsis* seedlings. The main response of *T. virens* to co-cultivation with *Arabidopsis* was the repression of gene expression. The biological processes of transport and metabolism of carbohydrates were downregulated, including a set of cell-wall-degrading enzymes putatively relevant for root-colonization. Repression of such genes reached their basal levels at later times of the interaction when genes belonging to the biological process of copper ion transport were induced, a necessary process providing copper as a cofactor for cell-wall degrading enzymes with auxiliary activities (AAs) class. RNA-Seq analyses showed the induction of a member of the

SNF2 family of chromatin remodelers/helicase-related proteins, which was named IPA-1 (Increased Protection of *Arabidopsis*-1). Sequence analyses of IPA-1 showed as its closest relatives members of the Rad5/Rad16- and SNF2-subfamilies; however, it grouped into a different clade. Although deletion of *ipa-1* in *T. virens* did not affect its growth, the antibiosis of Δ*ipa-1* culture filtrates showed a diminished effect against *Rhizoctonia solani* but remained unaltered against *Botrytis cinerea*. Triggering of the plant defense genes in plants treated with Δ*ipa-1* was higher, showing enhanced resistance against *Pseudomonas syringae* but not against *B. cinerea* as compared to wild type.

Keywords: chromatin-remodeling, SNF2 helicase-related proteins, RNA-Seq, transcriptomic response, *Trichoderma*-plant interaction, antibiosis, systemic acquired resistance, induced systemic resistance.

Introduction

The genus *Trichoderma* comprises ascomycete-filamentous fungi, cosmopolitan inhabitants of soil, decaying wood and vegetable matter. *Trichoderma* spp. can be isolated from crop fields, pastures, forests, salt marshes, prairies, and deserts (Kubicek et al. 2008). This may be owed to the diversified metabolic potential of *Trichoderma* spp. and their aggressive combative nature. The capacity of *Trichoderma* spp. as biological control agents of phytopathogenic fungi, oomycetes and nematodes has been well documented (Benítez et al. 2004). The biological control activity of *Trichoderma* spp. may involve one or more of the following processes: competition, antibiosis, and mycoparasitism (Howell 2003; Harman et al. 2004). Indirectly *Trichoderma* spp. are also

capable of protecting plants by triggering their defense mechanisms (Yedidia et al. 1999). In this regard, phytohormones and signal molecules play crucial roles in plant immunity, where salicylic acid (SA), jasmonates (JAs), ethylene (ET) and nitric oxide (NO) are the central players (Pieterse et al. 2009; Delledonne et al. 1998; Bellin et al. 2013). However, important data have shown that abscisic acid (ABA), auxins, gibberellins, cytokinins, and brassinosteroids, perform pivotal roles as well (Pieterse et al. 2009). Systemic acquired resistance (SAR) and induced systemic resistance (ISR) are plant defense responses, which are preconditioned by prior infection or treatment with the SA analogue benzothiadiazole (BTH) or JA/ET respectively, resulting in resistance against subsequent infections by pathogens. Triggering of SAR depends upon the phytohormone SA as a signal molecule, and is distinguished by the accumulation of genes encoding pathogenesis-related (PR) proteins (Durrant and Dong 2004; Van Loon 1975; Van Loon and Van Strien 1999). The SA-signaling cascade leads to a long-lasting disease resistance effect against biotrophic (i.e. *Hyaloperonospora arabidopsidis*) or hemibiotrophic (i.e. *Pseudomonas syringae*) phytopathogens (Heil and Bostock 2002; Pieterse et al. 2009). Moreover, ISR elicitation by soilborne beneficial microorganisms such as plant growth-promoting rhizobacteria and mycorrhizal fungi relies on the phytohormones JA and ET, as signal molecules, and is related to priming for augmented defense against a subsequent attack, rather than direct triggering of *PR* genes transcription (Van Wees et al. 2008; Pieterse et al. 2009). Nevertheless, after a subsequent attack, the ISR correlates with the enhanced transcription of the *HEL* (Potter et al. 1993), *CHIB* (Samac et al. 1990), and *PDF1.2* (Penninckx et al. 1996) genes, which code for a hevein-like protein, a chitinase, and a plant defensin, respectively. ISR is effective against necrotrophic phytopathogens (i.e. *Botrytis cinerea*) and herbivore insects (Pieterse et al. 2009; Van Oosten et al. 2008). Overall it is believed that the SA and JA/ET pathways are mutually exclusive (Felton et al. 1999; Kloek et al. 2001; Cui et al.

2005; Preston et al. 1999; Koornneef et al. 2008). However, several studies have shown a synergistic effect between these pathways. Simultaneous activation of the SA and JA/ET pathways in *Arabidopsis* results in enhanced resistance against the bacterial pathogen *Pseudomonas syringae* pv. *tomato* DC3000 (Van wees et al. 2000). Moreover, addition of higher concentration of SA and JA or prolonged treatments of *Arabidopsis* or tobacco plants resulted in antagonistic effect on transcription of *PDF1.2* and *Thi1.2* (Thionin), two JA responsive genes, and *PR-1a* (SA responsive gene) in a dose-dependent manner, whereas low concentrations resulted in increased accumulation of all three transcripts (Mur et al. 2006). Interestingly, the mycorrhiza-induced resistance (MIR) shares traits with pathogen-induced SAR and rhizobacterial ISR. MIR has been related to SAR-like priming for SA-dependent genes, but more frequently concurs with priming of JA-dependent defenses and cell wall defenses. In agreement with this, MIR confers protection against several biotrophic and necrotrophic pathogens, as well as herbivores and nematodes (Pozo and Azcón-Aguilar 2007; Cameron et al. 2013). Recent advances have rapidly unraveled that plant systemic acquired resistance (SAR)-related genes, as well as induced systemic resistance (ISR)-related genes are concurrently triggered upon plant root colonization by *Trichoderma* spp., conferring protection against pathogens with different lifestyle (Salas-Marina et al. 2011). *Trichoderma* strains also "prime" plants (Segarra et al. 2009; Salas-Marina et al. 2011; Mathys et al. 2012; Salas-Marina et al. 2015), which results in faster and/or enhanced induction of defense systems when plants are re-exposed to biotic or abiotic stresses (Goellner and Conrath 2008; Conrath et al. 2006). As in the case of *Pseudomonas simiae* (formerly *Pseudomonas fluorescens* WCS417), triggering of ISR by *Trichoderma* depends on the activation of the transcription factor MYB72 in the roots (Segarra et al. 2009). Interestingly, the volatile organic compounds (VOCs) produced by two *Trichoderma*-ISR inducing strains triggered the expression of *MYB72* as well as iron deficiency

responses in *Arabidopsis* roots, whereas in leaves VOCs primed the JA response against *B. cinerea*. Accordingly, it was suggested that *Trichoderma* VOCs modulate iron homeostasis in roots, promoting systemic priming trough JA dependent defenses in *Arabidopsis* (Martínez-Medina et al. 2017).

The activation of the mutually antagonistic SA and JA pathways by *Trichoderma* implies a cost in the plant ecological fitness causing a phenomenon known as cross-talk (Van Oosten et al. 2008). *Trichoderma*-plant interactions occur mainly in the rhizosphere, where the fungus produces and releases a diverse repertoire of molecules, microbe-associated molecular patterns (MAMP's), and/or elicitors of plant responses such as polygalacturonases (Thpg1) (Morán-Diez et al. 2009), xylanases (Eix) (Rotblat et al. 2002), cerato-platanins (Sm1/Epl1) (Djonović et al. 2006; Seidl et al. 2006), cellulases (Martinez et al. 2001), swollenins (Swo1) (Brotman et al. 2008), and hydrolases Thph1 and Thph2 (Saravanakumar et al. 2018). Plant growth promotion by *Trichoderma* has been studied for many years in numerous crops and model plants (Gravel et al. 2007; Hohmann et al. 2011; Bae et al. 2009; Mackenzie and Starman 1995; Salas-Marina et al. 2011). The arrival of the Genomic Era has facilitated the investigation of the *Trichoderma* transcriptome reprogramming in response to the presence of plants. One of the first studies reporting the reprogramming of *T. harzianum* T34 transcriptome during its co-culture with tomato seedlings highlighted the importance of the regulation of genes associated with redox reactions, lipid metabolism, detoxification, and sugar or amino-acid transport in this fungus (Chacón et al. 2007). A comparative analysis using high-density oligonucleotide microarrays contrasted the transcriptomic response of *T. harzianum* T34, *T. hamatum* T7 and *T. virens* T87 to the presence of tomato plants. That analysis showed that 3.15 % of the 12,428 genes predicted in the genome of

T. virens changed at least 2-fold in their expression when co-cultured with the plant (Rubio et al. 2012).

Recent lines of evidence have shown that chemical modifications of chromatin, a highly organized structure formed by DNA and histone proteins (Brosch et al. 2008), play pivotal roles in plant priming by beneficial microorganisms (Pieterse et al. 2014). Chromatin is not static and undergoes posttranslational chemical modifications at histone N-terminal tails, (Vaquero et al. 2003; Fry and Peterson 2001; Tsukiyama 2002), including methylation, acetylation, ubiquitylation, sumoylation and phosphorylation (Kouzarides 2007). Currently, chromatin dynamics in fungus-host interactions has gained attention (Gómez-Díaz et al. 2012; Ramirez-Prado et al. 2018; Gómez-Rodríguez et al. 2018; Estrada-Rivera et al. 2019). In addition to chromatin chemical modifications, chromatin-remodeling complexes, which includes members of the SNF2 family of helicase-related proteins, play important roles in chromatin structure and dynamic properties, therefore influencing a broad range of nuclear processes, including gene expression by either moving, ejecting or restructuring nucleosomes as well as functioning as transcription factors (Lusser and Kadonaga 2003; Martens and Winston 2003; Jansen and Verstrepen 2011). SNF2 family members can act as activators or repressors depending on the SNF2 component and the interacting proteins (Martens and Winston 2003).

SWI/SNF complexes are central players in different organisms such as yeast, animals, and plants (Hargreaves and Crabtree 2011; Euskirchen et al. 2012; Kadoch and Crabtree 2015; Sarnowska et al. 2016), nonetheless, relatively little is known about their functions in filamentous fungi. Research on the role of chromatin remodeling factors in fungus-host interactions is particularly scarce. In *Candida albicans*, an opportunistic human pathogen, the chromatin remodeling complex SWI/SNF is indispensable for appropriate hyphal development, virulence and azole resistance

(Mao et al. 2006; Liu and Myers 2017). To the best of our knowledge, the participation of a member of the family of SNF2 helicase-related proteins in fungus-plant interactions, notably of those fungi that confer beneficial effects to plants, such as *Trichoderma* spp. has remained largely unexplored.

Here, we focus on the analysis of the transcriptomic response of *Trichoderma virens* to the presence of *Arabidopsis thaliana* seedlings, showing that the carbohydrate metabolism and copper ion transport biological processes are significantly responsive to *Arabidopsis*. Validation of *T. virens* transcriptome by RT-qPCR showed high accuracy. Some of the validated genes have been shown to play pivotal roles in *Trichoderma*-Plant or pathogen-plant interactions, including signaling proteins such as Mitogen-Activated Protein Kinases (MAPK), histone methyltransferase and Ras-GTPases (Viterbo et al., 2005; Bi et al., 2013; Dautt-Castro et al., 2020), heat shock proteins (Montero-Barrientos et al., 2007), glycosyl hydrolases (Avni et al., 1994; Martínez et al., 2001; Rotblat et al., 2002; Moran-Diez et al., 2009), detoxifying enzymes (Dixit et al., 2011), and transporters of different types, among others. Transcriptomic analysis showed that the putative chromatin remodeler/transcription factor encoding gene *ipa-1* (increased protection of *Arabidopsis*-1) (TRIVIDRAFT_113458 [Genebank Accession number: XP_013960510; Kubicek et al., 2011]), closely related to members of the SNF2 family is induced during the interaction of *T. virens* with *Arabidopsis*. In this sense, the possible role of members of the IPA-1 subfamily in the *Trichoderma*-Plant interaction has not been explored, therefore we decided to investigate whether the *ipa-1* product was involved in the *T. virens*-*Arabidopsis* interaction. We found that a functional *ipa-1* gene is necessary for antibiosis against *Rhizoctonia solani* and properly turning-off the plant defense responses.

Results

Overview of transcriptome sequencing

To assess the transcriptional response of *T. virens* to the presence of *A. thaliana* seedlings, total RNA from the fungus was extracted at 48, 72 and 96 h of co-culture with the plant and validated by RT-qPCR of the *sm-1* (small protein -1) gene, which is induced by the presence of the plant (Djonović et al. 2006). *sm-1* expression was induced by the presence of *Arabidopsis*, showing its highest peak at 48 h of co-culture (Supplementary Fig. S1). Thereafter, eighteen RNA libraries from three biological replicates for each sample were sequenced using the SOLiD platform. In total, 219 million reads with an average length of 75 nucleotides (nt) were obtained (~16.4 Gb sequenced), with approximately 12 million reads per library. Reads of each library were mapped against the predicted genes on the *T. virens* genome V2, and those reads with multiple hits discarded (see materials and methods for details). Our results showed that roughly 98% of the mapped reads per library were aligned only once to the predicted genes (Table 1).

Pearson's correlation coefficient was high (an average of 0.95) between biological replicates of the same sample (Supplementary Fig. S2A). Furthermore, Multidimensional scaling (MDS) plot analysis showed the formation of four groups, suggesting that the samples contained in each group have similarities based on gene expression profiles. The first group consisted of *T. virens* control sample collected at 48 h of interaction with *Arabidopsis* (Tv_48h). The second group included the control samples of *T. virens* at 72 and 96 h of co-culture (Tv_72h and Tv_96h), whereas the third group included the *T. virens* sample growing in co-culture with *Arabidopsis* at 48 h (TvAt_48h). Interestingly, the fourth group was comprised of *T. virens-Arabidopsis* samples at 72 and 96 h (TvAt_72h and TvAt_96h) (Supplementary Fig. S2B).

Transcriptional response of *T. virens* to the presence of *Arabidopsis*

To identify the differentially expressed genes (DEG) in *T. virens* during its interaction with *Arabidopsis* at 48, 72 and 96 h, pairwise comparisons were carried out against the control samples (*T. virens* growing in 1× MS). Overall 691 different fungal genes responded to the presence of *Arabidopsis*, corresponding to 5.5% of the predicted genes in the fungus (Supplementary Table S4). As shown in Fig. 1A, the largest transcriptional response of *T. virens* during the interaction with *Arabidopsis* was observed at 48 h, involving mainly gene repression, with 518 differential expressed genes, of which, 434 were repressed and only 84 were induced. At 72 h of co-culture, 236 genes were differentially expressed including 138 induced and 98 repressed. Finally, at 96 h of interaction, only 153 genes were differentially expressed with 128 induced and 25 repressed (Supplementary Table S4). A comparison of upregulated genes showed that the transcriptional response of *T. virens* is specific to each time because only 31 genes were common to all-time points, whereas 44, 59 and 52 genes were specifically upregulated at 48, 72 and 96 h, respectively. However, a higher number of upregulated genes were shared at 72 and 96 h compared to 48 h, consistent with our MDS analysis. In contrast, the repression of *T. virens* genes during the interaction was more specific at early times. Interestingly, within the repressed genes 357 (77.9%) were specifically repressed at 48 h of interaction, compared to 25 (17.6%) and 8 (4.5%) at 72 and 96 h, respectively (Fig. 1B; Supplementary Table S4), suggesting that the transcriptional response of *T. virens* mainly involves gene repression at early stages of the interaction with the plant.

Hierarchical clustering by expression levels of 691 differentially expressed genes, grouped them in 7 clusters with similar expression profiles. Cluster 1 comprised 130 genes specifically repressed at 48 h of interaction, related to hydrolase activity of O-glycosyl compounds, carbohydrate

metabolic process, and glucosidase activity. Cluster 2 included 30 genes strongly repressed at 48 and 72 h, related to carbohydrate metabolic process, lysosome and vacuole organization, cellulose-binding and hydrolase activity of glycosyl compounds. Cluster 5 comprised 230 genes repressed exclusively at 48 h of interaction, which are involved in carbohydrate metabolic process, catalytic activity, oxidoreductase activity, and monooxygenase activity among others. Cluster 7 included 119 genes induced at 48, 72 and 96 h of co-culture, involved in copper ion transport, ferric chelate reductase activity, oxidoreductase activity, FAD and iron ion binding activity, among others. Cluster 3 formed by 81 slightly repressed genes at 48, 72 and 96 h contained genes related to catalase activity, carbohydrate metabolic process, hydrolase activity, and sugar symporter activity. Cluster 4 comprised 75 slightly induced genes at 72 h, including genes associated with transport and transcription factor activities. On the other hand, cluster 6 was formed by 53 genes specifically induced at 48 h of interaction, comprised genes encoding proteins related to SNF2-family domain proteins, oxidoreductase activity, metabolic process, and transcription factor activity among others (Fig. 1C; Table 2; Supplementary Tables S4 and S5); although, no GO terms were found enriched in this group.

To identify the biological processes involved in the *T. virens* response to the presence of *Arabidopsis*, functional annotation of differentially expressed genes based on Gene Ontology (GO) terms was performed. Subsequently, an enrichment analysis of the most specific GO terms using a Fisher's exact test (FDR <0.05) was carried out. A total of 87 GO terms were enriched during the *T. virens*-*Arabidopsis* interaction, of which 49 GO terms were enriched at 48 h, including 9 for upregulated and 40 for downregulated genes, whereas 21 were enriched at 72 h (13 for up- and 8 for downregulated genes) and only 17 GO terms were enriched in the upregulated genes at 96 h (Supplementary Fig. S3 and Supplementary Table S5). Analysis of the most specific GO terms

showed that the transcriptional response of *T. virens* at early times involved, mainly, repression of genes related to extracellular activity, lysosome activity, transport and metabolism of carbohydrates, sphingolipid metabolism, endochitinase activity, cellulose-binding, and hydrolysis of polysaccharides activity, among others. Moreover, four GO terms enriched for upregulated genes at 48 and 72 h of co-culture, included processes related to integral components of membrane, copper ion transport, and ferric-chelate reductase activity. Besides, the transcriptional response of *T. virens* at 96 h of interaction comprised the induction of genes related to copper ion transport, iron ion binding, ferric-chelate reductase activity, and flavin adenine dinucleotide binding (Supplementary Fig. S3; Supplementary Table S5). Additionally, GO terms enrichment analysis in the up- and downregulated genes shared between the time points evaluated (Fig. 1B) was performed. Our results showed six GO terms enriched for the 31 upregulated genes shared at all tested times, which are related to copper ion transport and oxidoreductase activity. On the other hand, the eleven downregulated genes shared in all tested times are related to carbohydrate metabolism processes. Moreover, the 61 downregulated genes shared between 48 and 72 h, and the 357 genes exclusive of 48 h are related to carbohydrate metabolic process, cellulose-binding, and hydrolase activity. For the rest of the interactions, no enriched GO terms were found (Supplementary Fig. S3; Supplementary Table S4).

Validation of RNA-seq by RT-qPCR

To validate the RNA-seq analysis, nineteen genes from distinct clusters, showing differential expression profiles at 48, 72 and 96 h of interaction were selected for RT-qPCR assessment as follows (Fig. 2; Supplementary Table S6): Cluster 1: *kin,* hypothetical- serine/threonine-protein kinase and *hsp23*, small heat-shock protein 23 (Fig. 2A and B). Cluster 2: *gh18,* glycoside

hydrolase family 18 protein; *gh7*, glycoside hydrolase family 7 and *gt4,* glycosyltransferase family 4 protein (Fig. 2C to E). Cluster 4: *oxrdtase,* hypothetical-oxidoreductase NAD-binding domain; *gst-2*, hypothetical-glutathione-S-transferase 2, and *aqp*, hypothetical-aquaporin (Fig. 2F to H). Cluster 6: *3hcd*-hypothetical-3-hydroxyacyl-CoA dehydrogenase; *set,* hypothetical-lysine methyltransferase [HMKT]; *ipa-1* a member of the SNF2 family of chromatin remodeler/helicase-related proteins (this work), and *tbrg-1* (*Trichoderma* Big Ras-GTPase), an hypothetical Ras GTPase (Dautt-Castro et al., 2020) (Fig. 2I to L). Cluster 7: *gst-1*, hypothetical-glutathione-S-transferase 1; *pfp*-1, hypothetical-glutamine amidotransferase; *TvHyd1*, hypothetical-hydrophobin; *pfp-2* hypothetical-glutamine amidotransferase; *slac-1*, hypothetical unknown uptake transporter; *nox*, hypothetical-ferric reductase-like transmembrane component and *rta1*, hypothetical-binding protein to unknown toxic compounds (Fig. 2M to S). Most of the RT-qPCR results agreed with the RNA-Seq analysis, except for *3hcd* that was induced at 48 and 72 h, and downregulated at 96, whereas data from RT-qPCR showed that it was slightly repressed at 48 h, therefore it was considered as a false positive (Fig. 2I). Thirteen genes showed the expression profile detected by RNA-seq in the different clusters, but to different extents (*kin, hsp23*, *gh7, oxrdtase*, *gst-2*, *aqp*, *set, tbrg-1, gst-1*, *pfp-1*, *TvHyd1*, *pfp-2*, and *rta1*) (Fig. 2A, B, D, F, G, H, J, L, M, N, O, P and S respectively), whereas the assessment of five genes by RT-qPCR (*gh18*, *gt4*, *ipa-1* [(increased protection of *Arabidopsis*-1]), *slac-1*, and *nox* showed their maximum change in expression at a different time point compared with RNA-seq, but their induction or repression was confirmed (Fig. 2C, E, K, Q, and R). Even though when the extent of modulation shown by RT-qPCR and RNA-seq may differ, the RT-qPCR expression patterns were consistent in 94.7% of the cases with the RNA-seq data.

TRIVIDRAFT_113458 belongs to a new subfamily of the SNF2 family of chromatin remodeler/helicase-related proteins

Many genes whose product functions are poorly described were regulated in *T. virens* during its interaction with *Arabidopsis*. Due to the lack of research on new fungal proteins in the different aspects of the biology of *Trichoderma* spp., such as chromatin remodeler/helicase-related proteins, we focused on the gene TRIVIDRAFT_113458 (Genebank Accession number: XP_013960510; Kubicek et al., 2011), which was considerably induced in the presence of *Arabidopsis*, and previously predicted to encode a protein belonging to the Rad5/16 like subfamily (Schmoll et al. 2016). This gene consists of 2,860 bp (base pairs) and codes for a 681 aa protein (Fig. 3A). Blastp and protein sequence alignment of TRIVIDRAFT_113458 with representative members of *S. cerevisiae*, *Neurospora crassa*, and *T. virens* showed specific hits and high identity against DEXH-box helicase domain of SHPRH-like proteins, spanning from amino acids (aa) 140 to 393, that are involved in ATP-dependent RNA or DNA unwinding (Fig. 3A and Supplementary Fig. S4). Furthermore, the analysis showed hits against the HepA domain (aa 189 to 678) of the Superfamily II DNA or RNA helicase, involved in transcription, replication, recombination and repair (Fig. 3A and Supplementary Fig. S4). TRIVIDRAFT_113458 aligned as well against SNF2_N, the SNF2 family N-terminal domain (covering from aa194 to 462) (Fig. 3A and Supplementary Fig S4), which is found in proteins participating in a variety of processes including transcription regulation, DNA repair, DNA recombination, and chromatin unwinding. Our protein of interest also contains a SF2_C_SNF domain, extended from aa 606 to 648 (Fig. 3A and Supplementary Fig. S4). SF2_C_SNF is a C-terminal helicase domain that belongs to the SNF family helicases of chromatin-remodeling factors that participate in recombination. They are DEAD-like helicases belonging to superfamily (SF)2, a diverse family of proteins involved in ATP-dependent RNA or

DNA unwinding. Also, TRIVIDRAFT_113458 showed a PLN03142 domain (Fig. 3A and Supplementary Fig. S4), which putatively belongs to the chromatin-remodeling complex ATPase chain (aa 195 to 659; Fig. 3A and Supplementary Fig. S4). Based on these analyses TRIVIDRAFT_113458 appears to be a versatile protein that could participate as chromatin remodeler, in transcription, recombination as well as in DNA repair. To investigate more in-depth all the characteristics shared with members of different subfamilies of the SNF2 family, a phylogenetic analysis using representative members of the yeast *S. cerevisiae* and *T. virens* was performed. Fig. 3B shows that TRIVIDRAFT_113458 grouped with hypothetical proteins, having as its closest relatives SNF2- and Rad5/16-subfamilies members (Fig. 3B). Based on these results, we classified TRIVIDRAFT_113458 as a member of a new subfamily of the SNF2-family of chromatin remodelers/helicase-related proteins, and named it IPA-1 (Increased Protection of *Arabidopsis*-1); therefore, its corresponding gene was named *ipa-1*.

IPA-1 does not participate in mycelial growth or conidiation in *T. virens*

Given that *ipa-1* was induced in response to the presence of *Arabidopsis* (Fig. 2K), which suggests it could play a major role in modulation of gene expression during the *T. virens*-*Arabidopsis* interaction, we deleted it in *T. virens* Gv29-8 wild-type background. We obtained several independent-hygromycin resistant colonies, which were tested by qPCR to corroborate the *ipa-1* and *hph* copy number (Supplementary Table S7). *ipa-1* was detected in the WT but not in Δ*ipa-1-23* and Δ*ipa-1-24* transformants, whereas the *hph* construct was found in a single copy in Δ*ipa-1-23* and Δ*ipa-1-24* and not detected in the wild-type (Supplementary Table S7). Neither of the mutants was affected in conidiation or radial growth under the growth conditions tested

(Supplementary Fig. S5). Because of the essentially identical phenotypes of Δ*ipa-1-23* and Δ*ipa-1-24*, we continued working only with the Δ*ipa-1-23* mutant, unless otherwise specified.

Lack of *ipa-1* did not impair the ability of *T. virens* to grow over *R. solani* or *B. cinerea*

To determine the capacity of Δ*ipa-1-23* to grow over *R. solani* or *B. cinerea*, dual cultures of the WT or Δ*ipa-1-23* strains with the two phytopathogens were performed. After seven days of confrontation, the WT and Δ*ipa-1-23* grew over the two phytopathogens with no detectable difference (Supplementary Fig. S6).

Mycelial free culture filtrates (MFCF) of Δ*ipa-1* showed diminished inhibition of *R. solani* radial growth

To better understand the role of IPA-1 in secondary metabolism and antimicrobial activity in *T. virens,* WT and Δ*ipa-1-23* were grown in PDB for 4 days. Then 1× PDA plates containing 40% of MFCF were prepared. Subsequently, a plug of actively growing mycelium of *R. solani* was inoculated on the PDA plates amended with MFCF or in PDA as control. Δ*ipa-1-23* MFCF provoked a reduction in growth inhibition on *R. solani* at 24, 48, 72 and 96 h (85.19 ± 2.80, 73.30 ± 0.81, 65.35 ± 1.21 and 52.85 ± 3.48) compared to the WT MFCF (86.90 ± 2.70, 82.82 ± 4.22, 78.09 ± 4.48 and 73.04 ± 5.11) (Fig. 4A and B). In contrast, there was no difference in the growth inhibition effect of the MFCFs of the WT and Δ*ipa-1-23* on *B. cinerea* (Supplementary Fig. S7).

Lack of *ipa-1* in *T. virens* resulted in enhanced plant protection against the bacterial phytopathogen *Pst* DC3000

To assess the role of IPA-1 in plant-growth promotion induced by *T. virens*, *Arabidopsis* seedlings were grown in pots and their roots inoculated with the WT or Δ*ipa-1-23* strains. Plants inoculated with Δ*ipa-1-23* showed statistically indistinguishable fresh and dry weights compared to those treated with the WT, indicating that lack of IPA-1 does not play a role in the plant growth-promoting activity of *T. virens* (Supplementary Fig. S8).

To assess whether IPA-1 is necessary to elicit plant defense responses by *T. virens,* the expression profiles of the *Arabidopsis* marker gene *PR-1a* (SAR), and the ET/JA and *Trichoderma* responsive gene *PDF1.2* (Estrada-Rivera et al. 2019) was assessed by RT-qPCR in co-cultures with the WT, Δ*ipa-1-23*, and Δ*ipa-1-24*. Expression of *PR-1a* and *PDF1.2* was induced by the WT, Δ*ipa-1-23*, and Δ*ipa-1-24*; however, the responses were stronger in plants treated with Δ*ipa-1-23* and Δ*ipa-1-24* (Fig. 5A to B).

Based on the expression profiles of *PR-1a* and *PDF1.2* in response to the Δ*ipa-1*, we asked whether the Δ*ipa-1-23* mutant provides more protection against the fungal and bacterial pathogens *B. cinerea* and *Pseudomonas syringae* pv tomato (*Pst* DC3000). Δ*ipa-1-23*-treated plants exhibited enhanced resistance to *Pst* DC3000 ($1.92\times10^7\pm5.49\times10^6$ CFU/ml) compared to control-plants ($1.27\times10^8\pm1.15\times10^7$ CFU/ml) and WT-treated plants ($8.70\times10^7\pm 1.01\times10^7$ CFU/ml) (Fig. 5E; Supplementary Fig. S9). WT- and Δ*ipa-1-23* treated plants and post infected with *B. cinerea* showed no significant differences in lesion covering only 7.8% and 7.02% of the leaf area, respectively. On the other hand, lesions in the control plants covered 49.2% of the leaf area (Fig. 5C to D).

Discussion

Here, we analyzed the transcriptomic response of *T. virens* to *Arabidopsis* plants. Enriched metabolic categories in the *T. virens* transcriptome indicated cellular processes prioritization in the presence of *Arabidopsis*. The biological processes of carbohydrate transport (48 h), and carbohydrate metabolic process (Cluster 2) were repressed in the fungus (48 and 72 h), as well as the molecular functions of monooxygenase, endochitinase, β-glucosidase, glucan endo-1,3-α-glucosidase, hydrolase activities as well as o-glycosyl compounds, and cellulose-binding. During plant root colonization *Trichoderma* deploys a broad array of specialized carbohydrate-active enzymes 'CAZymes' (Levasseur et al. 2013) for plant cell-wall polymer degradation, which can be classified as glycosyltransferases (GT), glycoside hydrolases (GH), polysaccharide lyases (PL), carbohydrate-binding modules (CBMs), carbohydrate esterases (CE), and auxiliary activities (AAs) (Martinez et al. 2008; Schmoll et al. 2016). In this analysis, a plethora of CAZymes encoding-genes was remarkably downregulated in *T. virens* at 48 h in the presence of *A. thaliana*, among them 45 putative glycoside hydrolases and four proteins containing putative carbohydrate-binding modules. Similar results were described for *Trichoderma parareesei* co-cultivated with tomato seedlings (Rubio et al. 2014). It is worth mentioning that inactive cell wall degrading enzymes (CWDE) such as xylanases and cellulases induce systemic responses (Avni et al., 1994; Martínez et al., 2001; Rotblat et al., 2002). Furthermore, the silencing of the endopolygalacturonase (PG) *Thpg1* gene of *Trichoderma harzianum* resulted in low PG activity, reduced ability to colonize tomato roots, and the induction of plant defense resistance was negatively affected (Moran-Diez et al., 2009). It is thus possible that *T. virens* downregulates the expression of CWDE encoding genes at the early stage of plant root colonization, to avoid the

production of DAMPs (Damage-Associated Molecular Patterns) or causing excessive damage to the plant tissue, as well as to avert the plant defense system since some such enzymes have demonstrated function as MAMPs (Avni et al., 1994; Martínez et al., 2001; Rotblat et al., 2002).

In addition, eighteen putative monooxygenases encoding-genes were downregulated in *T. virens* at 48 h of co-culture. In this regard, polysaccharide monooxygenases (PMOs), have recently been assigned to the novel category of AAs, which is divided into ten families or subfamilies according to the catalytic reaction mechanism or specific substrate (Levasseur et al. 2013). AAs generate highly reactive-non-specific free radicals, which in consequence impact the cleavage of carbon-carbon and ether inter-unit bonds using a metal-dependent oxidative mechanism (Beeson et al. 2011; Medie et al. 2012; Levasseur et al. 2008). The LPMO *Tr*AA9A from *Trichoderma reesei* a non-plant mutualistic *Trichoderma* species, enhances the activity of *Trichoderma logibrachiatum* cellulase *Tl*Cel7A on bacterial microcrystalline cellulose (BMCC). Pretreatment of BMCC with *Tr*AA9A potentiates the conversion of BMCC by a mixture of endoglucanase and β–glucosidase (Song et al., 2018). This fact paralleled with the downregulation of CWDE and LPMOs, supporting our hypothesis on the downregulation of such genes to reduce the production of DAMPs to avert the plant defense responses. In the phytopathogenic fungus *Magnaporthe oryzae*, silencing of the cellulase encoding genes GH6 and GH7 by RNAi led to the demonstration that they are essential for penetration of the host epidermis and further invasion by the fungus (Van Vu *et al*., 2012). The glycosyltransferases ZtGT2 and FgGT2 from the wheat pathogens *Zymoseptoria tritici* and *Fusarium graminearum* are required for hyphal growth on solid surfaces and virulence. Intriguingly, *Z. trici* strains lacking the *ZtGT2* gene showed constitutive expression of several transmembrane and secreted proteins such as LysM-domain chitin-binding virulence effector ZtLysM (King et al., 2017). Accordingly, the authors proposed that such glycosyltransferases may

also function in the synthesis of an unknown extracellular or outer cell wall polysaccharide which could be playing important roles in fungi-plant interactions, including mutualistic relationships (King et al., 2017). On the other hand, it would be reasonable to attribute the downregulation of the CAZymes to the lack of metals as cofactors for PMOs in the organism. Interestingly, the repression of genes, which code for enzymes involved in carbohydrate metabolism was only given at 48 h of interaction, remaining unchanged at later times when the biological process of copper ion transport, as well as the molecular functions of iron ion binding, ferric-chelate reductase, and copper ion transmembrane transport activities, were induced in *T. virens* by the presence of *Arabidopsis*, suggesting a role of these pathways in providing the necessary metals to *T. virens* PMOs. Furthermore, the repression of CAZymes during *T. virens* co-culture with *Arabidopsis* may also have been due to carbon catabolite repression (Ruijter and Visser 1997; Sun and Glass 2011; Nakari-Setälä et al. 2009). The reduction of CAZymes, which degrade the plant cell-wall in the *T. virens* transcriptome, may also be the result of a self-defense mechanism of *Trichoderma*, to escape or minimize the plant defense responses. Numerous studies have found a decreased repertory of carbohydrate-active enzymes in the genome of diverse biotrophic lifestyle microorganisms such as *Laccaria biccolor* (Martin et al. 2008), Périgord black truffle (Martin et al. 2010), *Hyaloperonospora arabidopsidis* (Baxter et al. 2010), and *Blumeria graminis* (Spanu et al. 2010). Authors of these studies claimed that the diminished number of CAZyme gives insights for the genetic basis of the most common symbiotic traits belonging to the oldest lineage of plant biotrophs. Unlike our data, during *T. harzianum* T34, *T. hamatum* T7 and *T. virens* T87 interaction with tomato triggers an important activation of fungal carbohydrate metabolism and transport processes (Rubio et al. 2012). However, it must be considered that the experimental conditions

used in each analysis, as co-culture times, host plant and *Trichoderma* species varied greatly between each study.

Genes of clusters 4 and 7, which were upregulated, and code for hydrophobins (putative MAMPs), proteins that participate in detoxifying the cells from reactive oxygen species (GST-1, and GST-2) (Osorio-Concepción et al., 2017) or xenobiotics (RTA1) (Soustre et al., 1996), where some of them have been shown to participate in *Trichoderma*-plant interaction or confer beneficial effects in transgenic plants (Dixit et al., 2011), were also regulated in *T. virens* by the presence of *Arabidopsis*. These facts may indicate that *T. virens* uses different anti-stress mechanisms during its interaction with *Arabidopsis* to protect itself from the plant hostile environment at the beginning of the interaction. On the contrary, the aquaporin, *aqp*-encoding gene was downregulated. Aquaporins are integral membrane proteins, functioning as gradient-driven water and/or solute channels across membranes, including ammonia, CO_2, hydrogen peroxide, and metalloids (Maurel and Plassard, 2011). Recently, it was reported that the overexpression of the aquaporin, AQP in *T. virens*, enhances plant growth and disease resistance against white mold in common bean seedlings (Brandão et al., 2019). Our results contrast with the results of Brandão et al. (2019) since they observed that the expression of AQP confers beneficial effects to plants, however, the expression of *aqp* was constitutive. Probably, *T. virens* downregulates the expression of *aqp* in the presence of *Arabidopsis* to prevent uncontrolled movements of solutes (ions and protons) that could damage the cells at the beginning of the interaction. The relevance of aquaporins during mycorrhizal fungus plant interaction for water and nutrient exchanges has been reported. A more complex role than just simply regulating plant water status has been proposed for aquaporins during arbuscular mycorrhizal symbiosis (Maurel and Plassard, 2011). Therefore, *T. virens* may regulate

differentially the expression of *aqp* at different stages of the interaction to succeed in plant root colonization and consequently confer beneficial effects to plants.

Proteins that participate in signal transduction such as serine/threonine kinases (Cluster 1), and histone methyltransferases and the founder member of a new family of Ras-GTPases, TBRG-1 (Cluster 6) (Dautt-Castro et al., 2020) were downregulated and upregulated respectively. In this regard, the role of a TMKA a MAPK was demonstrated to be indispensable in *T. virens* for the induction of systemic resistance in cucumber plants against the bacterial leaf pathogen *Pseudomonas syringae* pv. *lacrymans* (Viterbo *et al*., 2005). Recently, it was shown that the founding member of a new subfamily of Ras-GTPase, TBRG-1 (*Trichoderma* Big Ras-GTPase) participates in the biocontrol of *R. solani* against tomato seeds and seedlings, as well as in the recognition of the plant since mutants lacking the *tbrg-1* gene behave like a pathogen (Dautt-Castro *et al*., 2020). Even though *kin*-58043 is not a MAPK, it may have a similar regulatory function to that of TmkA, which led to its downregulation, possibly to avoid the activation of systemic resistance in *Arabidopsis* during the early stages of the interaction with *T. virens;* thus, allowing root colonization by the fungus. On the contrary, the upregulation of *tbrg-1* during the early stages of *Arabidopsis* root colonization by *T. virens* seems to be essential for the fungus to behave as a mutualistic microbe (Dautt-Castro et al., 2020). LAE1 a putative histone methyltransferase regulates positively the expression of seven genes encoding cellulases, auxiliary factors for cellulose degradation, β-glucosidases, and xylanases in *T. reesei* (Seiboth *et al*., 2012). In *Cochliobolus heterostrophus*, a maize fungal pathogen, Lae1-like methyltransferase negatively regulates T-toxin production, impacting adversely fungal virulence (Bi *et al*., 2013). Here, the histone lysine methyltransferase *set*-77874 is highly induced by the presence of *Arabidopsis*,

which may indicate an important role of lysine methylation at histone N-tails to establish a beneficial relationship.

Heat shock proteins (HSP) function as molecular chaperones under stressful conditions (heat shock, cold, UV light, etc.). Transgenic strains of *T. harzianum* bearing the heat shock protein 23 (*hsp23*) encoding gene from *T. virens* resulted in higher thermotolerance (Montero-Barrientos et al., 2007). *hsp23* grouped in cluster 1 was highly upregulated at 96 h during the *T. virens*-*Arabidopsis* interaction, which may indicate that HSP23 is necessary for the fungus during the early stages of the interaction, probably, to contend against the stressful conditions generated in the root epidermis.

TvHyd1 (143417), the orthologous to TasHyd1 from *Trichoderma asperellum* was upregulated in the presence of *Arabidopsis* (cluster 7), which together with other hydrophobins has been shown to play important roles in plant root colonization (Viterbo and Chet, 2006; Guzmán-Guzmán et al., 2017), promoting changes in root architecture that result in increased nutrient absorptive surface, enhancing plant growth (Samolski et al., 2012), as well as induction systemic disease resistance (Ruocco et al., 2015). These data together suggest that TvHyd1 could be important during *Arabidopsis* root colonization to confer the mentioned beneficial effects to the plants.

Cluster 7 also includes putative malate/sulfite transporter (*slac-1*) as well as the 7-amino cholesterol resistance-like protein-1 (*rta1*), which were upregulated in the presence of the plant. The metabolism of cysteine-rich compounds assimilated by fungi gives as byproduct sulfite, which is potentially toxic in the cell, where its excretion via an efflux pump is an option for detoxification. Interestingly, to grow within keratin, which has a high content of cysteine, dermatophytes secrete sulfite to reduce proteins by directly cleaving the disulfide bridges that make proteins accessible to various secreted endo- and exoproteases (Lechenne et al., 2007). Thus, SLAC-1 may participate

as a sulfite efflux pump to detoxify the *T. virens* cells as well as in sulphitolysis as complementary function to cleave the disulfide bridges of cysteine-rich proteins, making them more accessible to proteases.

7-aminocholesterol is a strong inhibitor of yeast and gram+-bacteria. In fungi, the RTA1 protein family comprises proteins bearing multiple transmembrane domains. It was proposed that these kinds of proteins might bind toxic substances (Soustre et al., 1996) therefore they could be implicated in the efflux of xenobiotics in *T. virens*.

Nowadays, there is much information regarding the different SNF2 subfamilies of chromatin remodeler/helicase-related proteins and their functions. This family of proteins is found in all eukaryotes from yeast to humans (Becker & Workman, 2013), including fungi of the genus *Trichoderma* (Schmoll et al., 2016). Members of this family of proteins regulate the structure and dynamics of chromatin, influencing many cellular processes (Becker & Workman, 2013). However, for filamentous fungi of the genus *Trichoderma*, analysis of the function of this family of proteins is scarce. Due to a lack of research on this family of proteins in *Trichoderma*, especially of those unexplored emerging subfamilies of the SNF2 family, we selected the *ipa-1* gene, which was upregulated in the presence of *Arabidopsis*. Here, we determined that IPA-1 belongs to a new subfamily of the SNF2 family of chromatin remodeler/helicase-related proteins, whose closest members belong to the Rad5/Rad16- and SNF2-subfamilies (Fig. 3 and Supplementary Fig. S4). This subfamily of SNF2 nucleosome chromatin remodeler/helicase factors could remodel nucleosomes located at regulatory elements on DNA; thus, modulating gene expression by either moving, ejecting or restructuring nucleosomes or through the exchange of histone variants. IPA-1 subfamily members may also have an impact on chromatin organization independent of their remodeler/helicase activities due to their different functional domains (Fig. 3). The functional

domains found in IPA-I and their relatives suggest they interact with DNA and histones, which could alter DNA-histone interactions in target nucleosomes to allow the entry or exit of coactivator and/or corepressors. Furthermore, remodeling activities are usually linked with other processes including histone modifications or RNA metabolism to assemble stable, epigenetics states.

The antagonistic activity of *T. virens* has been widely recognized, an analysis of >1,100 *Trichoderma* strains belonging to 75 species, demonstrated that all tested *Trichoderma* species possess potential mycoparasitic activity against three different fungal phytopathogens *Alternaria alternata*, *B. cinerea* and *Sclerotinia sclerotiorum* (Druzhinina et al. 2011). Interestingly, we found that MFCF from *ipa-1* lacking strains, showed a diminished antimicrobial effect on *R. solani*, but did not affect their activity against *B. cinerea.* The poor *R. solani* radial growth inhibition by Δ*ipa-1* MFCF, suggests that the mutant is affected in the production of a metabolite(s) important to inhibit or kill *R. solani*, but not *B. cinerea*. A plausible explanation is that IPA-1 regulates negatively a repressor of specific secondary metabolism-related genes, mainly those involved in the synthesis of antimicrobial compounds. Probably, IPA-1 acts by remodeling the nucleosomes or participating as a transcription factor or both at the repressor promoter, thereby allowing diminished transcription of the repressor messenger, whose product will impact on the promoters of specific secondary metabolism-related genes. Recently, it has been documented that chromatin modifications are relevant for the regulation of genes involved in secondary metabolism in *Trichoderma* (Gómez-Rodríguez et al. 2018; Osorio-Concepción et al. 2017; Estrada-Rivera et al. 2019).

As far as we know this is one of the first analyses of a mutant of *T. virens* affected in a protein with putative functions as chromatin remodeler/transcription factor/DNA repair and its impact and involvement in plant responses, including plant growth promotion, induction of genes involved in

systemic resistance, and plant protection against *B. cinerea* and *P. syringae*. Our data showed that lack of *ipa-1* caused overexpression of *PDF1.2* and *PR-1a* in *Arabidopsis*. Consequently, plants root-inoculated with Δ*ipa-1* and challenged with *P. syringae* showed greater resistance to the pathogen compared with plants treated with the WT. The general question in chromatin remodelers/transcription factor analysis is whether these proteins may be acting as specific or general transcriptional regulators (Tsukiyama 2002; Kwon and Wagner 2007). Our work demonstrates that *ipa-1* deletion does not affect cell viability, conidiation, development, antagonism, antibiosis against *B. cinerea,* and plant growth promotion activity in *T. virens*, pointing to specific regulation in the organism. Furthermore, our data suggest that IPA-1 may function as a negative regulator of genes that encode proteins that induce the SAR and ISR pathways. Interestingly, an opposite outcome was determined in a mutant of a histone deacetylase (HDA-2) of *T. atroviride*, which was incapable of triggering a plant-defense response, and thus affecting the plant-protection effect against *B. cinerea* and *P. syringae* (Estrada-Rivera et al. 2019).

It has been demonstrated that SWI/SNF components can act as repressors of gene transcription (Martens and Winston 2003). In this regard, chromatin immunoprecipitation (ChIP) trials showed that SWI/SNF members are physically located at repressed promoters (Martens and Winston 2002; Battaglioli et al. 2002; Chi et al. 2002; Archacki et al. 2017). The specificity of the *T. virens* IPA-1 resembles that observed in *A. thaliana*, where an SWI/SNF class chromatin remodeling ATPase SPLAYED (SYD), function as a downstream regulator of gene expression of the ET and JA pathways (Walley et al. 2008). SYD is necessary for plant-resistance against *B. cinerea* but not versus *P. syringae* (Walley et al. 2008).

In summary, we have shown that *T. virens* responds transcriptionally to the presence of *Arabidopsis*, mainly by gene repression. Carbohydrate transport and carbohydrate metabolic

biological processes were downregulated, whereas copper ion transport was upregulated. Interestingly, some chromatin modification and remodeling proteins encoding genes were induced, such as SET (histone methyltransferase) and SNF2-family-related proteins (*ipa-1*). Mutants lacking *ipa-1* showed a WT phenotype regarding colony growth and conidiation as well as mycoparasitism against *B. cinerea*. Antibiosis of Δ*ipa-1* MFCF against *R. solani* showed a diminished activity compared with the WT MFCF. Plants treated with Δ*ipa-1* showed upregulation of *PR-1a* and *PDF1.2* genes, which resulted in enhanced resistance against *Pst* DC3000, but not against *B. cinerea*. Our work highlights the importance of chromatin remodeling complexes members in secondary metabolism as well as in the interaction of *T. virens* with plants.

Materials and Methods

Organisms and growth conditions

Arabidopsis thaliana ecotype Col-0 was utilized throughout this work. *Arabidopsis* seeds were disinfected by soaking in 75% ethanol for 3 min, washed with 10% bleach (HOCl) in water for 7 min, and rinsed three times with sterile distilled water. Seeds were incubated at 4 °C for 2 days for stratification and then germinated and grown on 0.7× MS (PhytoTechnology Laboratories®) (Murashige and Skoog, 1962) agar plates under 16/8 h light/dark photoperiod at 22 °C ± 1 °C, 65% relative humidity, and 150 μmol $m^{-2}s^{-1}$ light. *T. virens* Gv29-8 WT (wild-type) (Baek and Kenerley 1998), its isogenic mutants Δ*ipa-1-23,* Δ*ipa-1-24* (this work), *Botrytis cinerea* B05.10 (Amselem et al. 2011), and *Rhizoctonia solani* AG-4 were used in this study. All fungal strains were usually grown at 28 °C on potato dextrose agar (PDA; DIFCO), under a 12/12 h light/dark

regime. The bacterium *Pseudomonas syringae* pv. *tomato,* strain DC3000 (Cuppels 1986) was grown at 28 °C in Kings B medium (King et al. 1954), supplemented with rifampicin 50 μg/ml.

RNA-Seq libraries preparation and sequencing

To construct the RNA-seq libraries, twenty ten-day-old *Arabidopsis* plants grown on 1× MS plates were inoculated at the root tips with mycelial plugs of *T. virens* WT (wild-type), and mycelia were collected using a scalpel at 48, 72 and 96 h of co-culture. *T. virens* growing in 1× MS plates were used as control. Mycelial samples were frostbitten in liquid nitrogen and laid up at -80 ºC until their processing. Total RNA was extracted by the TRIzol method (Invitrogen) following the protocol recommended by the manufacturer. DNA contamination was eliminated with TURBO DNase (Life Technologies). RNA samples were quantified by determining the absorbance ratio at A260/280 and A260/230 using an Epoch Spectrophotometer (Biotek). RNA samples were evaluated for quality and quantity utilizing an Agilent 2100 Bioanalyzer (Agilent Technologies). RNA having an integrity number (RIN) ≥ 8.0 was used for librarie's construction. RNA-Seq libraries construction and sequencing were carried out at the Genomics Core Facility at the Laboratorio Nacional de Genómica para la Biodiversidad (LANGEBIO), CINVESTAV (Irapuato, Gto., Mexico). RNA-seq libraries were prepared from 3 biological RNA replicates for each treatment and sequenced in the SOLiD platform (Sequencing by Oligonucleotide Ligation and Detection; Applied Biosystems) following the manufacturer's instructions. The raw reads were deposited in the NCBI Gene Expression Omnibus (GEO) under the accession number GSE125225.

RNA-Seq data analysis and functional annotation

Sequenced reads (csfasta and qual files) were converted into the fastq format using the SOLiD system XSQ Tools and solid2fastq.pl script, and their quality was checked with FastQC (Andrews, 2010). Reads were mapped against the predicted genes of the *T. virens* genome version 2 (Kubicek et al. 2011) using the Burrows-Wheeler Aligner (BWA) software (Li and Durbin 2009) allowing 4% of mismatches. Visualization and quantification of reads per gene were carried out utilizing the Tablet tool (Milne et al. 2009), and only reads with unique hits were maintained and used for the quantification of the number of reads per gene. The *T. virens* gene IDs used in this work correspond to the protein IDs published in the *T. virens* genome version 2 (https://genome.jgi.doe.gov/TriviGv29_8_2/TriviGv29_8_2.home.html). Correlation and biological coefficient of variation between samples and biological replicates were determined with a Pearson´s correlation and multidimensional scaling analyzes (MDS) using the normalized expression data by trimmed mean of M values (TMM). Only the biological replicates with a Pearson´s correlation factor ≥ 0.9 between them were considered for subsequent analyzes. Almost all biological replicates showed a Pearson´s correlation factor greater than 0.9, except for the biological replicate 2 of *T. virens* growing in MS media (Tv48h.2). To assess the transcriptional response of *T. virens* to the presence of *A. thaliana*, we determined the differentially expressed genes by comparison of *T. virens* growing in MS medium versus *T. virens* in co-culture with *A. thaliana* at 48, 72 and 96 h, using the edgeR package (Robinson et al. 2010), applying a statistical methods based on pairwise comparisons and a common dispersion calculated as suggested by edgeR manual. Genes exhibiting a false discovery rate (FDR) ≤ 0.05 and a $\log_2$ Fold Change ≥ 1 ($\log_2$FC) were taken as differentially expressed genes (DEG). Functional annotation of DEG based on gene ontology terms and the enrichment analysis (Fisher´s exact test, FDR < 0.05) were performed using BLAST2GO suite (Conesa et al. 2005). Hierarchical clustering of DEG and the

heat map of the GO terms enriched were created using the hclust (method= "Ward.D") and heatmap.2 packages in R (v3.5.1).

Sequences analysis and phylogeny

NCBI-Blastp was conducted to assess the sequences similarity of IPA-1 (Increased Protection of *Arabidopsis*-1) with other proteins belonging to the SNF2 family. Conserved regions and motif elements were detected by multiple sequence alignment using ClustalW (ExPASy) and MEME-SUITE (Bailey et al., 2009). The *T. atroviride* IPA-1 amino acid sequence was aligned against representative proteins of the SNF2 family from *Saccharomyces cerevisiae*, *Neurospora crassa* and *T. virens*, using MUSCLE with default settings. A Phylogenetic tree was constructed using MEGAX by the neighbor-joining method (Saitou and Nei, 1987) with bootstrap support with 1500 replicates (Kumar et al., 2016). The evolutionary distances were computed using the Poisson correction method (Zuckerkandl and Pauling, 1965). The edition of the tree was performed on the interactive tree of life (iTOL) v3 (Letunic and Bork, 2016).

RNA-Seq validation by RT-qPCR

Transcriptome validation of *T. virens* was performed with one of the biological replicates. cDNA was synthesized using 5 µg of total RNA with SuperScript II Reverse Transcriptase (Invitrogen), following the manufacturer's recommendations. The oligonucleotides were designed utilizing the software Primer 3 (Applied Biosystems) (Supplementary Table S1), and the RT-qPCR (Reverse transcription polymerase chain reaction) reactions were executed using the Fast Syber Green Master Mix kit (Applied Biosystem), with 100 ng of cDNA from each sample. The Abiprism 7500

Fast Real-Time PCR system (Applied Biosystem) was used throughout the study. The gene *tef-1* was utilized as a reference gene for the normalization of the measured genes, by using the formula $2^{-\Delta\Delta Ct}$ (Livak and Schmittgen 2001).

Generation of *T. virens* protoplast

Protoplast were generated as described elsewhere (Baek and Kenerley 1998) with modifications: 1×10^8 conidia/ml were inoculated in 100 ml of PDYCB medium (per liter: 24 g potato dextrose broth, 2 g yeast extract, 1.2 g casein hydrolysate medium) and incubated for three days under shaking at 250 rpm at 28 °C. Mycelium was filtrated and collected, washed with 0.01 M phosphate buffer (pH 7.2), and 0.5 g suspended in osmoticum (50 mM $CaCl_2$, 0.5 M mannitol, 50 mM MES, pH 5.5) with 15 mg/ml lytic enzymes of *Trichoderma harzianum* (Sigma, L1412). The blend was incubated for 5 h at 28 °C under mild stirring. For protoplast regeneration, a selective medium (potato dextrose broth DIFCO™, 0.8% Agarose (Nara Biotec), and 0.5 M sucrose) amended with 200 µg/ml hygromycin was used.

Genetic transformation of *T. virens* and gene replacement mutants screening

Primer design and deletion of *ipa-1* gene were performed accordingly to double-joint PCR technology (Yu et al. 2004). In the first round of PCR, the 5 '(5'SNF2-F and 5' SNF2-R-Fusion) and 3' (3 SNF2-F-Fusion and 3 SNF2-R) modules of *ipa-1* were amplified with specific primers (Supplementary Table S2), using *T. virens* genomic DNA as a template. The *hph* cassette was amplified by PCR with DJhph-F and DJhph-R specific primers (Supplementary Table S2) using pCB1004 vector bearing the *hph* as the template (Carrol et al. 1994). In the second round of PCR,

the three fragments were fused and then purified with Wizard® Genomic DNA Purification Kit. Herculase II Fusion DNA Polymerase (Agilent) was used for all PCR reactions following the manufacturer's recommendations. The final product was used to transform *T. virens* WT protoplasts. Monosporic transformants were obtained by three consecutive transfers of a single colony to PDA amended with 200 µg/ml hygromycin. Total DNA from hygromycin-resistant transformants was submitted to PCR using 5'SNF2-F'-Upstream and 3'SNF2-R'-Downstream oligonucleotides (Supplementary Table S2), corresponding to sequences on the genome ≈100 bp up and downstream of the 5' and 3' modules used in the fusion PCR, respectively, to evaluate the appropriate gene replacement events. To assess the gene replacement, and to test for ectopic insertions of *hph* construct in the *T. virens* genome, DNA from the selected transformants was submitted to qPCR utilizing specific primers for *hph* and *ipa-1* (Supplementary Table S2). Copy number of *hph* and *ipa-1* of the hygromycin-resistant colonies was calculated using the $2^{-\Delta\Delta Ct}$ procedure (Bubner and Baldwin 2004).

Phenotype analysis and conidia quantification

WT, Δ*ipa-1-23* and Δ*ipa-1-24* strains were grown on Petri dishes containing PDA at 28 ºC under a 12/12 h light-dark photoperiod. Phenotypes of each strain were photographed and evaluated qualitatively by visual inspection every 24 h. Radial growth of the colonies was also measured every 24 h and conidia were harvested with water and quantified at 24, 48, 72 and 96 h with a Neubauer chamber (Marienfeld, Germany) under the microscope (Zeiss).

Dual cultures of *T. virens* WT and Δ*ipa-1* strains versus *R. solani* and *B. cinerea*

WT and Δ*ipa-1-23* capability to grow over the phytopathogens *R. solani* and *B. cinerea* were assessed in dual cultures confrontation assays. Agar plugs of actively growing mycelia of *T. virens* strains and the phytopathogens were placed on the opposite sides of PDA plates and incubated at 28 °C by 7 days and photographed.

Antimicrobial activity of *T. virens* WT and Δ*ipa-1* mycelium-free culture filtrates (MFCF) versus *R. solani* and *B. cinerea*

To determine the antifungal properties of Δ*ipa-1-23* MFCF versus *R. solani* and *B. cinerea*, 1×10^7 conidia/ml of the WT or Δ*ipa-1-23* were inoculated in 150 ml of PDB and grown by four days at 28 °C and 200 rpm. Subsequently, the WT and Δ*ipa-1-23* cultures were filtered under vacuum through 0.20 µm filter papers, and 1× PDA plates containing 40% (v/v) of the MFCF were prepared. Mycelial slices of *R. solani* or *B. cinerea* were placed at one edge of the 1× PDA plates containing 40% and incubated at 28 °C for 4 and 7 days respectively. Phytopathogens growing on 1× PDA plates without MFCF served as controls. Colony diameters were measured every 24 h.

Effect of Δ*ipa-1* on plant growth promotion

Arabidopsis seeds were sown in flowerpots including peat moss (Lambert peat moss) as substrate and stratified at 4 °C for 2 days, and allowed to germinate at 22 °C ± 1 °C, 65% relative humidity, and 150 µmol $m^{-2}s^{-1}$ light. One-day-old plants were transplanted into pots containing sterile peat moss and grown under 16/8 h light/dark photoperiod at 22 °C ± 1 °C, 65% relative humidity, and 150 µmol $m^{-2}s^{-1}$ light. One week later, 15 *Arabidopsis* plants were root inoculated with 500 µl of 1×10^6 conidia/ml of the WT or Δ*ipa-1-23* in 0.3× MS. Plants growing without the fungi were used

as control. Three weeks postinoculation, fresh and dry weights were assessed on an analytical scale.

Expression assessment of defense-related genes in *Arabidopsis* seedlings treated with the WT or Δ*ipa-1*

Arabidopsis seedlings were grown 9 days on Petri dishes containing 1× MS. Thereafter, seedlings were root-inoculated with disks of actively growing mycelium of the WT, Δ*ipa-1-23*, and Δ*ipa-1-24*. Plants were harvested at 0, 48, 72, and 96 h of hpi (hours post-inoculation), frostbitten in liquid nitrogen and laid up at -80 ºC till total RNA extraction. Plants growing without the fungi were used as controls. Extraction of total RNA, cDNA synthesis, and RT-qPCR were assessed as described above, and specific oligonucleotides were used for the PCR (Supplementary Table S3). Relative expression was standardized versus the level of *ACT2* by the $2^{-\Delta\Delta Ct}$ procedure (Livak and Schmittgen 2001).

***Botrytis cinerea* pathogenesis assay**

Ten-day-old *Arabidopsis* seedlings were root treated with 500 µl of 1×10^6 conidia/ml of *T. virens* or Δ*ipa-1-23* in 0.3× MS liquid medium. Two weeks later *Arabidopsis* leaves were infected with 10 µl of a conidial suspension 5×10^5 conidia/ml of *B. cinerea* in the following inoculation buffer (per 40 ml of the stock solution: 1.37 g Sucrose, 400 µl 1M KH_2PO_4, 80 µl of 12.5% Tween 20). Lesion sizes of infected plants were quantitatively measured at 6 dpi using ImageJ software [http://rsb.info.nih.gov/ij/index.html].

Pseudomonas syringae Pst DC3000 infection assay

Ten-day-old *Arabidopsis* seedlings were root inoculated with 500 µl of a 1×10^6 conidia/ml of *T. virens* or Δ*ipa-1-23* in 0.3× MS liquid medium. After two weeks, three leaves per seedling were infiltrated with *Pst* DC3000 in 10 mM $MgCl_2$ (OD_{600} = 0.0004) using a needleless syringe. Twelve leaves of control and treated plants were collected at 0 and 3 dpi, and ground in 10 mM $MgCl_2$. Samples were diluted serially and plated onto King's B medium amended with the suitable antibiotics to determine the colony-forming unit (CFU).

Acknowledgments

This work was supported by grants CB-2008-01-103733 and IFC-2016-1538 to SC-F. ME-R, JJG-N and OGR-P are indebted to CONACYT for doctoral fellowships. MD-C is supported by IFC-2016-1538. The authors wish to thank Nicolás Gómez-Hernández for his technical support.

Literature Cited

Amselem, J., Cuomo, C. A., van Kan, J. A. L., Viaud, M., Benito, E. P., Couloux, A., Coutinho, P. M., de Vries, R. P., Dyer, P. S., Fillinger, S., Fournier, E., Gout, L., Hahn, M., Kohn, L., Lapalu, N., Plummer, K. M., Pradier, J. M., Quévillon, E., Sharon, A., Simon, A., Have, A., Tudzynski, B., Tudzynski, P., Wincker, P., Andrew, M., Anthouard, V., Beever, R. E., Beffa, R., Benoit, I., Bouzid, O., Brault, B., Chen, Z., Choquer, M., Collémare, J., Cotton, P., Danchin, E. G., Da Silva, C., Gautier, A., Giraud, C., Giraud, T., Gonzalez, C.,

Grossetete, S., Güldener, U., Henrissat, B., Howlett, B. J., Kodira, C., Kretschmer, M., Lappartient, A., Leroch, M., Levis, C., Mauceli, E., Neuvéglise, C., Oeser, B., Pearson, M., Poulain, J., Poussereau, N., Quesneville, H., Rascle, C., Schumacher, J., Ségurens, B., Sexton, A., Silva, E., Sirven, C., Soanes, D. M., Talbot, N. J., Templeton, M., Yandava, C., Yarden, O., Zeng, Q., Rollins, J. A., Lebrun, M. H., and Dickman, M. 2011. Genomic Analysis of the Necrotrophic Fungal Pathogens Sclerotinia sclerotiorum and Botrytis cinerea. PLoS Genet. 7:1–27

Archacki, R., Yatusevich, R., Buszewicz, D., Krzyczmonik, K., Patryn, J., Iwanicka-Nowicka, R., Biecek, P., Wilczynski, B., Koblowska, M., Jerzmanowski, A., and Swiezewski, S. 2017. Arabidopsis SWI/SNF chromatin remodeling complex binds both promoters and terminators to regulate gene expression. Nucleic Acids Res. 45:3116–3129

Avni, A., Bailey, B.A., Mattoo, A.K., and Anderson J.D., 1994. Induction of ethylene biosynthesis in Nicotiana tabacum by a Trichoderma viride xylanase is correlated to the accumulation of 1- aminocyclopropane-1-carboxylic acid (ACC) synthase and ACC oxidase transcripts. Plant Physiol. 106:1049e1055

Bae, H., Sicher, R. C., Kim, M. S., Kim, S.-H., Strem, M. D., Melnick, R. L., and Bailey, B. A. 2009. The beneficial endophyte Trichoderma hamatum isolate DIS 219b promotes growth and delays the onset of the drought response in Theobroma cacao. J. Exp. Bot. 60:3279–3295

Baek, J. M., and Kenerley, C. M. 1998. The arg2 gene of Trichoderma virens: cloning and development of a homologous transformation system. Fungal Genet. Biol. 23:34–44

Bailey, T.L., Boden, M., Buske, F.A., Frith, M., Grant, C.E., Clementi, L., Ren, J., Li, W.W.,

Noble, W.S. 2009. MEME SUITE: tools for motif discovery and searching. Nucleic Acids Res. 37, W202–W208

Bateman, A., Coin, L., Durbin, R., Finn, R. D., Hollich, V., Griffiths-Jones, S., Khanna, A., Marshall, M., Moxon, S., Sonnhammer, E. L. L., Studholme, D. J., Yeats, C., and Eddy, S. R. 2004. The Pfam protein families database. Nucleic Acids Res. 32:D138–D141

Battaglioli, E., Andrés, M. E., Rose, D. W., Chenoweth, J. G., Rosenfeld, M. G., Anderson, M. E., Rosenfeld, M. G., and Mandel, G. 2002. REST Repression of Neuronal Genes Requires Components of the hSWI·SNF Complex. J. Biol. Chem. 277:41038–41045

Baxter, L., Tripathy, S., Ishaque, N., Boot, N., Cabral, A., Kemen, E., Thines, M., Ah-Fong, A., Anderson, R., Badejoko, W., Bittner-Eddy, P., Boore, J. L., Chibucos, M. C., Coates, M., Dehal, P., Delehaunty, K., Dong, S., Downton, P., Dumas, B., Fabro, G., Fronick, C., Fuerstenberg, S. I., Fulton, L., Elodie, G., Govers, F., Hughes, L., Humphray, S., Jiang, R. H. Y., Judelson, H., Kamoun, S., Kyung, K., Meijer, H., Minx, P., Paul, M., Joanne, N., Phuntumart, V., Qutob, D., Rehmany, A., Rougon-Cardoso, A., Ryden, P., Torto-Alalibo, T., Studholme, D., Wang, Y., Win, J., Wood, J., Clifton, S. W., Rogers, J., Ackerveken, G. Van den, Jones, J. D. G., McDowell, J. M., Beynon, J., and Tyler, B. M. 2010. Signatures of Adaptation to Obligate Biotrophy in the Hyaloperonospora arabidopsidis Genome. Science (80-.). 330:1549–1551

Becker, P. B. and Workman, J. L. 2013. Nucleosome remodeling and epigenetics. Cold Spring Harbor Perspectives in Biology. 5: a017905

Beeson, W. T., Phillips, C. M., Cate, J. H. D., and Marletta, M. A. 2011. Oxidative Cleavage of Cellulose by Fungal Copper-Dependent Polysaccharide Monooxygenases. J. Am. Chem.

Soc. 134:890–892

Bellin, D., Asai, S., Delledonne, M., and Yoshioka, H. 2013. Nitric oxide as a mediator for defense responses. Mol. Plant. Microbe Interact. 26:271-277.

Benítez, T., Rincón, A. M., Limón, M. C., and Codón, A. C. 2004. Biocontrol mechanisms of Trichoderma strains. Int. Microbiol. 7:249–260

Bi, Q., Wu, D., Zhu, X., and Turgeon, B. G. 2013. Cochliobolus heterostrophus Llm1–a Lae1-like methyltransferase regulates T-toxin production, virulence, and development. Fungal Genet. Biol. 51:21-33

Brandão, R. S., Qualhato, T. F., Valdisser, P. A. M. R., de CB Côrtes, M. V., Vieira, P. M., Silva, R. N., ... and Ulhoa, C. J. 2019. Evaluation of Trichoderma harzianum mutant lines in the resistance induction against white mold and growth promotion of common bean. BioRxiv. 713776

Brosch, G., Loidl, P., and Graessle, S. 2008. Histone modifications and chromatin dynamics: A focus on filamentous fungi. FEMS Microbiol. Rev. 32:409–439

Brotman, Y., Briff, E., Viterbo, A., and Chet, I. 2008. Role of Swollenin, an Expansin-Like Protein from Trichoderma, in Plant Root Colonization. Plant Physiol. 147:22–32

Bubner, B., and Baldwin, I. T. 2004. Use of real-time PCR for determining copy number and zygosity in transgenic plants. Plant Cell Rep. 23:263–271

Cameron, D. D., Neal, A. L., van Wees, S. C., and Ton, J. 2013. Mycorrhiza-induced resistance: more than the sum of its parts?. Trends Plant Sci. 18:539-545

Cervantes-Badillo, M. G., Muñoz-Centeno, T., Uresti-Rivera, E. E., Argüello-Astorga, G. R.,

and Casas-Flores, S. 2013. The Trichoderma atroviride photolyase-encoding gene is transcriptionally regulated by non-canonical light response elements. FEBS J. 280:3697–708

Chacón, M. R., Rodríguez-galán, O., Benítez, T., Sousa, S., Rey, M., Llobell, A., and Delgado-Jarana, J. 2007. Microscopic and transcriptome analyses of early colonization of tomato roots by Trichoderma harzianum. Int. Microbiol. 10:19–27

Chi, T. H., Wan, M., Zhao, K., Taniuchi, I., Chen, L., Littman, D. R., and Crabtree, G. R. 2002. Reciprocal regulation of CD4/CD8 expression by SWI/SNF-like BAF complexes. Nature. 418:195–199

Conesa, A., Götz, S., García-Gómez, J. M., Terol, J., Talón, M., and Robles, M. 2005. Blast2GO: A universal tool for annotation, visualization and analysis in functional genomics research. Bioinformatics. 21:3674–3676

Conrath, U., Beckers, G. J. M., Flors, V., García-Agustín, P., Jakab, G., Mauch, F., Newman, M.-A., Pieterse, C. M. J., Poinssot, B., Pozo, M. J., Pugin, A., Schaffrath, U., Ton, J., Wendehenne, D., Zimmerli, L., and Mauch-Mani, B. 2006. Priming: getting ready for battle. Mol. Plant. Microbe. Interact. 19:1062–71

Cui, J., Bahrami, A. K., Pringle, E. G., Hernandez-Guzman, G., Bender, C. L., Pierce, N. E., and Ausubel, F. M. 2005. Pseudomonas syringae manipulates systemic plant defenses against pathogens and herbivores. Proc. Natl. Acad. Sci. 102:1791–1796

Cuppels, D. A. 1986. Generation and characterization of Tn5 insertion mutations in Pseudomonas syringae pv. tomato. Appl. Environ. Microbiol. 51:323–327

Dautt-Castro, M., Estrada-Rivera, M., Olguin-Martínez, I., del Carmen Rocha-Medina, M., Islas-Osuna, M. A., and Casas-Flores, S. 2020. TBRG-1 a Ras-like protein in Trichoderma virens involved in conidiation, development, secondary metabolism, mycoparasitism, and biocontrol unveils a new family of Ras-GTPases. Fungal Genet. Biol. 136: 103292

Delledonne, M., Xia, Y., Dixon, R. A., and Lamb, C. 1998. Nitric oxide functions as a signal in plant disease resistance. Nature. 394:585-588

Ding, S., Mehrabi, R., Koten, C., Kang, Z., Wei, Y., Seong, K., Kistler, H. C., and Xu, J. R. 2009. Transducin beta-like gene FTL1 is essential for pathogenesis in fusarium graminearum. Eukaryot. Cell. 8:867–876

Dixit P., Mukherjee P. K., Ramachandran V., and Eapen S. 2011. Glutathione transferase from Trichoderma virens enhances cadmium tolerance without enhancing its accumulation in transgenic Nicotiana tabacum. PLoS One 6:e16360

Djonović, S., Pozo, M. J., Dangott, L. J., Howell, C. R., and Kenerley, C. M. 2006. Sm1, a proteinaceous elicitor secreted by the biocontrol fungus Trichoderma virens induces plant defense responses and systemic resistance. Mol. Plant. Microbe. Interact. 19:838–53

Druzhinina, I. S., Seidl-Seiboth, V., Herrera-Estrella, A., Horwitz, B. a, Kenerley, C. M., Monte, E., Mukherjee, P. K., Zeilinger, S., Grigoriev, I. V, and Kubicek, C. P. 2011. Trichoderma: the genomics of opportunistic success. Nat. Rev. Microbiol. 9:749–59

Durrant, W. E., and Dong, X. 2004. Systemic Acquired Resistance. Annu. Rev. Phytopathol. 42:185–209

Estrada-Rivera, M., Rebolledo-Prudencio, O. G., Pérez-Robles, D. A., Rocha-Medina, M. del C.,

González-López, M. del C., and Casas-Flores, S. 2019. Trichoderma histone deacetylase HDA-2 modulates multiple responses in Arabidopsis. Plant Physiol. 179:1343–1361

Euskirchen, G., Auerbach, R. K., and Snyder, M. 2012. SWI/SNF chromatin-remodeling factors: Multiscale analyses and diverse functions. J. Biol. Chem. 287:30897–30905

Felton, G. W., Korth, K. L., Bi, J. L., Wesley, S. V., Huhman, D. V., Mathews, M. C., Murphy, J. B., Lamb, C., and Dixon, R. A. 1999. Inverse relationship between systemic resistance of plants to microorganisms and to insect herbivory. Curr. Biol. 9:317–320

Fry, C. J., and Peterson, C. L. 2001. Chromatin remodeling enzymes: Who's on first? Curr. Biol. 11:185–197

Goellner, K., and Conrath, U. 2008. Priming: It's all the world to induced disease resistance. Sustain. Dis. Manag. a Eur. Context. :233–242

Gómez-Díaz, E., Jordà, M., Peinado, M. A., and Rivero, A. 2012. Epigenetics of Host-Pathogen Interactions: The Road Ahead and the Road Behind. PLoS Pathog. 8

Gómez-Rodríguez, E. Y., Uresti-Rivera, E. E., Patrón-Soberano, O. A., Islas-Osuna, M. A., Flores-Martínez, A., Riego-Ruiz, L., Rosales-Saavedra, M. T., and Casas-Flores, S. 2018. Histone acetyltransferase TGF-1 regulates Trichoderma atroviride secondary metabolism and mycoparasitism. PLoS One. 13:1–23

Gravel, V., Antoun, H., and Tweddell, R. J. 2007. Growth stimulation and fruit yield improvement of greenhouse tomato plants by inoculation with Pseudomonas putida or Trichoderma atroviride: Possible role of indole acetic acid (IAA). Soil Biol. Biochem. 39:1968–1977

Hargreaves, D. C., and Crabtree, G. R. 2011. ATP-dependent chromatin remodeling: Genetics, genomics and mechanisms. Cell Res. 21:396–420

Harman, G. E., Howell, C. R., Viterbo, A., Chet, I., and Lorito, M. 2004. Trichoderma species—opportunistic, avirulent plant symbionts. Nat. Rev. Microbiol. 2:43

Heil, M., and Bostock, R. M. 2002. Induced systemic resistance (ISR) against pathogens in the context of induced plant defences. Ann. Bot. 89:503–512

Hohmann, P., Jones, E. E., Hill, R. a, and Stewart, A. 2011. Understanding Trichoderma in the root system of Pinus radiata: associations between rhizosphere colonisation and growth promotion for commercially grown seedlings. Fungal Biol. 115:759–67

Jansen, A., and Verstrepen, K. J. 2011. Nucleosome Positioning in Saccharomyces cerevisiae. Microbiol. Mol. Biol. Rev. 75:301–320

Kadoch, C., and Crabtree, G. R. 2015. Mammalian SWI/SNF chromatin remodeling complexes and cancer: Mechanistic insights gained from human genomics. Sci. Adv. 1:1–17

King, E. O., Ward, M. K., and Raney, D. E. 1954. Two simple media for the demonstration of pyocyanin and fluorescin. J. Lab. Clin. Med. 44:301–307

Kloek, A. P., Verbsky, M. L., Sharma, S. B., Schoelz, J. E., Vogel, J., Klessig, D. F., and Kunkel, B. N. 2001. Resistance to Pseudomonas syringae conferred by an Arabidopsis thaliana coronatine-insensitive (coi1) mutation occurs through two distinct mechanisms. Plant J. 26:509–522

Koornneef, A., Leon-Reyes, A., Ritsema, T., Verhage, A., Otter, F. C. Den, Van Loon, L. C., and Pieterse, C. M. J. 2008. Kinetics of Salicylate-Mediated Suppression of Jasmonate

Signaling Reveal a Role for Redox Modulation. Plant Physiol. 147:1358–1368

Kouzarides, T. 2007. Chromatin Modifications and Their Function. Cell. 128:693–705

Kubicek, C. P., Herrera-Estrella, A., Seidl-Seiboth, V., Martinez, D. a, Druzhinina, I. S., Thon, M., Zeilinger, S., Casas-Flores, S., Horwitz, B. a, Mukherjee, P. K., Mukherjee, M., Kredics, L., Alcaraz, L. D., Aerts, A., Antal, Z., Atanasova, L., Cervantes-Badillo, M. G., Challacombe, J., Chertkov, O., McCluskey, K., Coulpier, F., Deshpande, N., von Döhren, H., Ebbole, D. J., Esquivel-Naranjo, E. U., Fekete, E., Flipphi, M., Glaser, F., Gómez-Rodríguez, E. Y., Gruber, S., Han, C., Henrissat, B., Hermosa, R., Hernández-Oñate, M., Karaffa, L., Kosti, I., Le Crom, S., Lindquist, E., Lucas, S., Lübeck, M., Lübeck, P. S., Margeot, A., Metz, B., Misra, M., Nevalainen, H., Omann, M., Packer, N., Perrone, G., Uresti-Rivera, E. E., Salamov, A., Schmoll, M., Seiboth, B., Shapiro, H., Sukno, S., Tamayo-Ramos, J. A., Tisch, D., Wiest, A., Wilkinson, H. H., Zhang, M., Coutinho, P. M., Kenerley, C. M., Monte, E., Baker, S. E., and Grigoriev, I. V. 2011. Comparative genome sequence analysis underscores mycoparasitism as the ancestral life style of Trichoderma. Pages R40 in: Genome biology, BioMed Central Ltd.

Kubicek, C. P., Komon-Zelazowska, M., and Druzhinina, I. S. 2008. Fungal genus Hypocrea/Trichoderma: from barcodes to biodiversity. J. Zhejiang Univ. Sci. B. 9:753–63

Kumar, S., Stecher, G., Tamura, K. 2016. MEGA7: Molecular Evolutionary Genetics Analysis Version 7.0 for Bigger Datasets. Mol. Biol. Evol. 33: 1870–1874

Kwon, C. S., and Wagner, D. 2007. Unwinding chromatin for development and growth : a few genes at a time. 23

Lechenne, B., Reichard, U., Zaugg, C., Fratti, M., Kunert, J., Boulat, O., and Monod, M. 2007.

Sulphite efflux pumps in Aspergillus fumigatus and dermatophytes. Microbiology. 153: 905-913

Letunic, I., Bork, P. 2016. Interactive tree of life (iTOL) v3: an online tool for the display and annotation of phylogenetic and other trees. Nucleic Acids Res. 44: W242–W245

Levasseur, A., Drula, E., Lombard, V., Coutinho, P. M., and Henrissat, B. 2013. Expansion of the enzymatic repertoire of the CAZy database to integrate auxiliary redox enzymes. Biotechnol. Biofuels. 6:1–14

Levasseur, A., Piumi, F., Coutinho, P. M., Rancurel, C., Asther, M., Delattre, M., Henrissat, B., Pontarotti, P., Asther, M., and Record, E. 2008. FOLy: An integrated database for the classification and functional annotation of fungal oxidoreductases potentially involved in the degradation of lignin and related aromatic compounds. Fungal Genet. Biol. 45:638–645

Li, H., and Durbin, R. 2009. Fast and accurate short read alignment with Burrows-Wheeler transform. Bioinformatics. 25:1754–1760

Liu, Z., and Myers, L. C. 2017. Candida albicans Swi/Snf and Mediator Complexes Differentially Regulate Mrr1- Induced MDR1 Expression and Fluconazole Resistance. Antimicrob. Agents Chemother. 61:1–24

Livak, K. J., and Schmittgen, T. D. 2001. Analysis of relative gene expression data using real-time quantitative PCR and the 2(-Delta Delta C(T)) Method. Methods. 25:402–408

Lusser, A., and Kadonaga, J. T. 2003. Chromatin remodeling by ATP-dependent molecular machines. BioEssays. 25:1192–1200

Mackenzie, A. J. and, and Starman, T. W. 1995. Enhanced Root and Shoot Growth of

Chrysanthemum Cuttings Propagated with the Fungus Trichoderma harzianum. HORTSCIENCE. 30:496–498

Mao, X., Cao, F., Nie, X., Liu, H., and Chen, J. 2006. The Swi/Snf chromatin remodeling complex is essential for hyphal development in Candida albicans. FEBS Lett. 580:2615–2622

Martens, J. A., and Winston, F. 2002. Evidence that Swi/Snf directly represses transcription in S. cerevisiae. Genes Dev. 16:2231–2236

Martens, J. A., and Winston, F. 2003. Recent advances in understanding chromatin remodeling by Swi/Snf complexes. Curr. Opin. Genet. Dev. 13:136–142

Martin, F., Aerts, A., Ahrén, D., Brun, A., Danchin, E. G. J., Duchaussoy, F., Gibon, J., Kohler, A., Lindquist, E., Pereda, V., Salamov, A., Shapiro, H. J., Wuyts, J., Blaudez, D., Buée, M., Brokstein, P., Canbäck, B., Cohen, D., Courty, P. E., Coutinho, P. M., Delaruelle, C., Detter, J. C., Deveau, A., DiFazio, S., Duplessis, S., Fraissinet-Tachet, L., Lucic, E., Frey-Klett, P., Fourrey, C., Feussner, I., Gay, G., Grimwood, J., Hoegger, P. J., Jain, P., Kilaru, S., Labbé, J., Lin, Y. C., Legué, V., Le Tacon, F., Marmeisse, R., Melayah, D., Montanini, B., Muratet, M., Nehls, U., Niculita-Hirzel, H., Secq, M. P. O. Le, Peter, M., Quesneville, H., Rajashekar, B., Reich, M., Rouhier, N., Schmutz, J., Yin, T., Chalot, M., Henrissat, B., Kües, U., Lucas, S., Van De Peer, Y., Podila, G. K., Polle, A., Pukkila, P. J., Richardson, P. M., Rouzé, P., Sanders, I. R., Stajich, J. E., Tunlid, A., Tuskan, G., and Grigoriev, I. V. 2008. The genome of Laccaria bicolor provides insights into mycorrhizal symbiosis. Nature. 452:88–92

Martin, F., Kohler, A., Murat, C., Balestrini, R., Coutinho, P. M., Jaillon, O., Montanini, B.,

Morin, E., Noel, B., Percudani, R., Porcel, B., Rubini, A., Amicucci, A., Amselem, J., Anthouard, V., Arcioni, S., Artiguenave, F., Aury, J. M., Ballario, P., Bolchi, A., Brenna, A., Brun, A., Buée, M., Cantarel, B., Chevalier, G., Couloux, A., Da Silva, C., Denoeud, F., Duplessis, S., Ghignone, S., Hilselberger, B., Iotti, M., Marçais, B., Mello, A., Miranda, M., Pacioni, G., Quesneville, H., Riccioni, C., Ruotolo, R., Splivallo, R., Stocchi, V., Tisserant, E., Viscomi, A. R., Zambonelli, A., Zampieri, E., Henrissat, B., Lebrun, M. H., Paolocci, F., Bonfante, P., Ottonello, S., and Wincker, P. 2010. Périgord black truffle genome uncovers evolutionary origins and mechanisms of symbiosis. Nature. 464:1033–1038

Martínez-Medina, A., Van Wees, S. C. M., and Pieterse, C. M. J. 2017. Airborne signals from Trichoderma fungi stimulate iron uptake responses in roots resulting in priming of jasmonic acid-dependent defences in shoots of Arabidopsis thaliana and Solanum lycopersicum. Plant. Cell Environ. 40:2691–2705

Martinez, C., Blanc, F., Le Claire, E., Besnard, O., Nicole, M., and Baccou, J. C. 2001. Salicylic acid and ethylene pathways are differentially activated in melon cotyledons by active or heat-denatured cellulase from Trichoderma longibrachiatum. Plant Physiol. 127:334–344

Martinez, D., Berka, R. M., Henrissat, B., Saloheimo, M., Arvas, M., Baker, S. E., Chapman, J., Chertkov, O., Coutinho, P. M., Cullen, D., Danchin, E. G. J., Grigoriev, I. V., Harris, P., Jackson, M., Kubicek, C. P., Han, C. S., Ho, I., Larrondo, L. F., De Leon, A. L., Magnuson, J. K., Merino, S., Misra, M., Nelson, B., Putnam, N., Robbertse, B., Salamov, A. A., Schmoll, M., Terry, A., Thayer, N., Westerholm-Parvinen, A., Schoch, C. L., Yao, J., Barbote, R., Nelson, M. A., Detter, C., Bruce, D., Kuske, C. R., Xie, G., Richardson, P., Rokhsar, D. S., Lucas, S. M., Rubin, E. M., Dunn-Coleman, N., Ward, M., and Brettin, T. S. 2008. Genome sequencing and analysis of the biomass-degrading fungus Trichoderma

reesei (syn. Hypocrea jecorina). Nat. Biotechnol. 26:553–560

Mathys, J., De Cremer, K., Timmermans, P., Van Kerckhove, S., Lievens, B., Vanhaecke, M., Cammue, B. P. a, and De Coninck, B. 2012. Genome-Wide Characterization of ISR Induced in Arabidopsis thaliana by Trichoderma hamatum T382 Against Botrytis cinerea Infection. Front. Plant Sci. 3:1–25

Maurel, C., and Plassard, C. 2011. Aquaporins: for more than water at the plant-fungus interface? New Phytol. 190: 815-817

Medie, F. M., Davies, G. J., Drancourt, M., and Henrissat, B. 2012. Genome analyses highlight the different biological roles of cellulases. Nat. Rev. Microbiol. 10:227–234

Milne, I., Bayer, M., Cardle, L., Shaw, P., Stephen, G., Wright, F., and Marshall, D. 2009. Tablet-next generation sequence assembly visualization. Bioinformatics. 26:401–402

Montero-Barrientos M, Cardoza R, Gutiérrez S, Monte E, Hermosa R. 2007. The heterologous overexpression of hsp23, a small heat-shock protein gene from Trichoderma virens, confers thermotolerance to T. harzianum. Curr Genet. 52:45–53

Morán-Diez, E., Hermosa, R., Ambrosino, P., Cardoza, R. E., Gutiérrez, S., Lorito, M., and Monte, E. 2009. The ThPG1 Endopolygalacturonase Is Required for the Trichoderma harzianum–Plant Beneficial Interaction. Mol. Plant-Microbe Interact. MPMI. 22:1021–31

Mur, L. A. J., Kenton, P., Atzorn, R., Miersch, O., and Wasternack, C. 2006. The Outcomes of Concentration-Specific Interactions between Salicylate and Jasmonate Signaling Include Synergy, Antagonism, and Oxidative Stress Leading to Cell Death. Plant Pathol. J. 140:249–262

Nakari-Setälä, T., Paloheimo, M., Kallio, J., Vehmaanperä, J., Penttilä, M., and Saloheimo, M. 2009. Genetic modification of Carbon Catabolite Repression in Trichoderma reesei for Improved Protein Production. Appl. Environ. Microbiol. 75:4853–4860

Osorio-concepción, M., Cristóbal-mondragón, G. R., Gutiérrez-Medina, B., and Casas-Flores, S. 2017. Histone Deacetylase HDA-2 Regulates Trichoderma atroviride Growth, Conidiation, Blue Light Perception, and Oxidative Stress Responses. Appl. Environ. Microbiol. 83:1–19

Penninckx, I. A. M. A., Eggermont, K., Terras, F. R. G., Thomma, B. P. H. J., Samblanx, G. W. De, Buchala, A., Metraux, J.-P., Manners, J. M., and Broekaert, W. F. 1996. Pathogen-Induced Systemic Activation of a Plant Defensin Gene in Arabidopsis Follows a Salicylic Acid-Independent Pathway. Plant Cell Online. 8:2309–2323

Pieterse, C. M. J., Leon-Reyes, A., Van der Ent, S., and Van Wees, S. C. M. 2009. Networking by small-molecule hormones in plant immunity. Nat. Chem. Biol. 5:308–16

Pieterse, C. M., Zamioudis, C., Berendsen, R. L., Weller, D. M., Van Wees, S. C., and Bakker, P. A. 2014. Induced systemic resistance by beneficial microbes. Annu. Rev. Phytopathol. 52:347-375

Potter, S., Uknes, S., Lawton, K., Winter, A., Chandler, D., DiMaio, J., Novitzky, R., Ward, E., and Ryals, J. 1993. Regulation of a Hevein-like gene in Arabidopsis. Mol. Plant. Microbe. Interact. 6:680–685

Pozo, M. J., and Azcón-Aguilar, C. 2007. Unraveling mycorrhiza-induced resistance. Curr. Opin. Plant Biol. 10:393-398

Preston, C. A., Lewandowski, C., Enyedi, A. J., and Baldwin, I. T. 1999. Tobacco mosaic virus

inoculation inhibits wound-induced jasmonic acid-mediated responses within but not between plants. Planta. 209:87–95

Ramirez-Prado, J. S., Piquerez, S. J. M., Bendahmane, A., Hirt, H., Raynaud, C., and Benhamed, M. 2018. Modify the Histone to Win the Battle: Chromatin Dynamics in Plant–Pathogen Interactions. Front. Plant Sci. 9:1–18

Robinson, M. D., McCarthy, D. J., and Smyth, G. K. 2010. edgeR: a Bioconductor package for differential expression analysis of digital gene expression data. Bioinformatics. 26:139–40

Rotblat, B., Enshell-Seijffers, D., Gershoni, J. M., Schuster, S., and Avni, A. 2002. Identification of an essential component of the elicitation active site of the EIX protein elicitor. Plant J. 32:1049–55

Rubio, M. B., Domínguez, S., Monte, E., and Hermosa, R. 2012. Comparative study of Trichoderma gene expression in interactions with tomato plants using highdensity oligonucleotide microarrays. Microbiology. 158:119–128

Rubio, M. B., Quijada, N. M., Pérez, E., Domínguez, S., Monte, E., and Hermosa, R. 2014. Identifying beneficial qualities of Trichoderma parareesei for plants. Appl. Environ. Microbiol. 80:1864–1873

Ruijter, G. J. G., and Visser, J. 1997. Carbon repression in Aspergilli. FEMS Microbiol. Lett. 151:103–114

Saitou, N., Nei, M. 1987. The neighbor-joining method: a new method for reconstructing phylogenetic trees. Mol. Biol. Evol. 4: 406–425

Salas-Marina, M. A., Isordia-Jasso, M. I., Islas-Osuna, M. A., Delgado-Sánchez, P., Jiménez-

Bremont, J. F., Rodríguez-Kessler, M., Rosales-Saavedra, M. T., Herrera-Estrella, A., and Casas-Flores, S. 2015. The Epl1 and Sm1 proteins from Trichoderma atroviride and Trichoderma virens differentially modulate systemic disease resistance against different life style pathogens in Solanum lycopersicum. Front. Plant Sci. 6:1–13

Salas-Marina, M. A., Silva-Flores, M. A., Uresti-Rivera, E. E., Castro-Longoria, E., Herrera-Estrella, A., and Casas-Flores, S. 2011. Colonization of Arabidopsis roots by Trichoderma atroviride promotes growth and enhances systemic disease resistance through jasmonic acid/ethylene and salicylic acid pathways. Eur. J. Plant Pathol. 131:15–26

Samac, D. A., Hironaka, C. M., Yallaly, P. E., and Shah, D. M. 1990. Isolation and characterization of the genes encoding basic and acidic chitinase in *Arabidopsis thaliana*. Plant Physiol. 93:907–914

Saravanakumar, K., Wang, S., Dou, K., Lu, Z., and Chen, J. 2018. Yeast two-hybrid and label-free proteomics based screening of maize root receptor to cellulase of Trichoderma harzianum. Physiol. Mol. Plant Pathol. 104:86–94

Sarnowska, E., Gratkowska, D. M., Sacharowski, S. P., Cwiek, P., Tohge, T., Fernie, A. R., Siedlecki, J. A., Koncz, C., and Sarnowski, T. J. 2016. The Role of SWI/SNF Chromatin Remodeling Complexes in Hormone Crosstalk. Trends Plant Sci. 21:594–608

Schmoll, M., Dattenböck, C., Carreras-Villaseñor, N., Mendoza-Mendoza, A., Tisch, D., Alemán, M. I., Baker, S. E., Brown, C., Cervantes-Badillo, M. G., Cetz-Chel, J., Cristobal-Mondragon, G. R., Delaye, L., Esquivel-Naranjo, E. U., Frischmann, A., Gallardo-Negrete, J. de J., García-Esquivel, M., Gomez-Rodriguez, E. Y., Greenwood, D. R., Hernández-Oñate, M., Kruszewska, J. S., Lawry, R., Mora-Montes, H. M., Muñoz-Centeno, T., Nieto-

Jacobo, M. F., Nogueira Lopez, G., Olmedo-Monfil, V., Osorio-Concepcion, M., Piłsyk, S., Pomraning, K. R., Rodriguez-Iglesias, A., Rosales-Saavedra, M. T., Sánchez-Arreguín, J. A., Seidl-Seiboth, V., Stewart, A., Uresti-Rivera, E. E., Wang, C.-L., Wang, T.-F., Zeilinger, S., Casas-Flores, S., and Herrera-Estrella, A. 2016. The Genomes of Three Uneven Siblings: Footprints of the Lifestyles of Three Trichoderma Species. Microbiol. Mol. Biol. Rev. 80:205–327

Segarra, G., Ent, S. Van der, Trillas, I., and Pieterse, C. M. J. 2009. MYB72, a node of convergence in induced systemic resistance triggered by a fungal and a bacterial beneficial microbe. Plant Biol. 11:90–96

Seidl, V., Marchetti, M., Schandl, R., Allmaier, G., and Kubicek, C. P. 2006. Epl1, the major secreted protein of Hypocrea atroviridis on glucose, is a member of a strongly conserved protein family comprising plant defense response elicitors. FEBS J. 273:4346–59

Siersleben, S., Penselin, D., Wenzel, C., Albert, S., and Knogge, W. 2014. PFP1, a Gene Encoding an Epc-N Domain-Containing Protein, Is Essential for Pathogenicity of the Barley Pathogen Rhynchosporium commune. Eukaryot. Cell. 13:1026–1035

Song, B., Li, B., Wang, X., Shen, W., Park, S., Collings, C., ... and Ding, S. Y. (2018). Real-time imaging reveals that lytic polysaccharide monooxygenase promotes cellulase activity by increasing cellulose accessibility. Biotechnol. Biofuels, 11: 41

Soustre, I., Letourneux, Y., and Karst, F. 1996. Characterization of the Saccharomyces cerevisiae RTA1 gene involved in 7-aminocholesterol resistance. Curr. Genet. 30: 121-125

Spanu, P. D., Abbott, J. C., Amselem, J., Burgis, T. A., Soanes, D. M., Stüber, K., Van Themaat, E. V. L., Brown, J. K. M., Butcher, S. A., Gurr, S. J., Lebrun, M. H., Ridout, C. J., Schulze-

Lefert, P., Talbot, N. J., Ahmadinejad, N., Ametz, C., Barton, G. R., Benjdia, M., Bidzinski, P., Bindschedler, L. V., Both, M., Brewer, M. T., Cadle-Davidson, L., Cadle-Davidson, M. M., Collemare, J., Cramer, R., Frenkel, O., Godfrey, D., Harriman, J., Hoede, C., King, B. C., Klages, S., Kleemann, J., Knoll, D., Koti, P. S., Kreplak, J., López-Ruiz, F. J., Lu, X., Maekawa, T., Mahanil, S., Micali, C., Milgroom, M. G., Montana, G., Noir, S., O'Connell, R. J., Oberhaensli, S., Parlange, F., Pedersen, C., Quesneville, H., Reinhardt, R., Rott, M., Sacristán, S., Schmidt, S. M., Schön, M., Skamnioti, P., Sommer, H., Stephens, A., Takahara, H., Thordal-Christensen, H., Vigouroux, M., Weßling, R., Wicker, T., and Panstruga, R. 2010. Genome Expansion and Gene Loss in Powdery Mildew Fungi Reveal Tradeoffs in extreme Parasitism. Science (80-.). 330:1543–1546

Studt, L., Schmidt, F. J., Jahn, L., Sieber, C. M. K., Connolly, L. R., Niehaus, E. M., Freitag, M., Humpf, H. U., and Tudzynski, B. 2013. Two histone deacetylases, FfHda1 and FfHda2, are important for Fusarium fujikuroi secondary metabolism and virulence. Appl. Environ. Microbiol. 79:7719–7734

Sun, J., and Glass, N. L. 2011. Identification of the CRE-1 Cellulolytic Regulon in Neurospora crassa. PLoS One. 6

Tsukiyama, T. 2002. THE IN VIVO FUNCTIONS OF ATP-DEPENDENT CHROMATIN-REMODELLING FACTORS. 3:422–429

Van Loon, L. C. 1975. Polyacrylamide disk electrophoresis of the soluble leaf proteins from Nicotiana tabacum var. "Samsun" and "Samsun NN" III. Influence of temperature and virus strain on changes induced by tobacco mosaic virus. Physiol. Plant Pathol. 6:289–300

Van Loon, L. C., and Van Strien, E. a. 1999. The families of pathogenesis-related proteins, their

activities, and comparative analysis of PR-1 type proteins. Physiol. Mol. Plant Pathol. 55:85–97

Van Oosten, V. R., Bodenhausen, N., Reymond, P., Van Pelt, J. A., Van Loon, L. C., Dicke, M., and Pieterse, C. M. J. 2008. Differential Effectiveness of Microbially Induced Resistance Against Herbivorous Insects in Arabidopsis. Mol. Plant-Microbe Interact. 21:919–930

Vaquero, A., Loyola, A., and Reinberg, D. 2003. The Constantly Changing Face of Chromatin. Sci. Aging Knowl. Environ. :1–16

Van wees, S. C. M. van, Swart, E. A. M. de, Pelt, J. A. van, Loon, L. C. van, and Pieterse, C. M. J. 2000. Enhancement of induced disease resistance by simultaneous activation of salicylate- and jasmonate-dependent defense pathways in Arabidopsis thaliana. Proc. Natl. Acad. Sci. 97:8711–8716

Van wees, S. C. Van, Ent, S. Van der, and Pieterse, C. M. 2008. Plant immune responses triggered by beneficial microbes. Curr. Opin. Plant Biol. 11:443–448

Viterbo, A., Harel, M., Horwitz, B. A., Chet, I., and Mukherjee, P. K. 2005. Trichoderma mitogen-activated protein kinase signaling is involved in induction of plant systemic resistance. Appl. Environ. Microbiol. 71:6241-6246

Walley, J. W., Rowe, H. C., Xiao, Y., Chehab, E. W., Kliebenstein, D. J., Wagner, D., and Dehesh, K. 2008. The Chromatin Remodeler SPLAYED Regulates Specific Stress Signaling Pathways. PLoS Pathog. 4:1–8

Yedidia, I., Benhamou, N., and Chet, I. 1999. Induction of Defense Responses in Cucumber Plants (Cucumis sativus L .) by the Biocontrol Agent Trichoderma harzianum. Appl.

Environ. Microbiol. 65:1061–1070

Yu, J.-H., Hamari, Z., Han, K.-H., Seo, J.-A., Reyes-Domínguez, Y., and Scazzocchio, C. 2004. Double-joint PCR: a PCR-based molecular tool for gene manipulations in filamentous fungi. Fungal Genet. Biol. 41:973–81

Zuckerkandl, E., Pauling, L. 1965. Evolutionary divergence and convergence in proteins, in: Evolving Genes and Proteins. Elsevier, pp. 97–166

Table 1. Alignment statistics to the predicted genes in *T. virens* genome V2

Sample	Total reads	Total mapped reads	%[a]	Filtered reads with unique hit	%[b]
Tv_48h.1	10,638,040	4,742,561	44.6	4,670,185	98.5
Tv_48h.2	8,948,382	3,998,400	44.7	3,922,972	98.1
Tv_48h.3	16,175,272	6,620,122	40.9	6,513,256	98.4
Tv_72h.1	10,587,525	4,420,421	41.8	4,339,249	98.2
Tv_72h.2	9,912,382	4,174,130	42.1	4,105,547	98.4
Tv_72h.3	29,927,732	11,940,497	39.9	11,735,297	98.3
Tv_96h.1	10,585,610	4,368,118	41.3	4,280,790	98.0
Tv_96h.2	9,116,693	3,728,951	40.9	3,657,705	98.1
Tv_96h.3	16,969,904	6,738,066	39.7	6,627,744	98.4
TvAt_48h.1	9,373,116	3,947,810	42.1	3,871,633	98.1
TvAt_48h.2	9,660,475	4,087,627	42.3	4,010,811	98.1
TvAt_48h.3	12,018,028	5,140,130	42.8	5,048,819	98.2
TvAt_72h.1	11,255,646	4,760,713	42.3	4,667,094	98.0
TvAt_72h.2	9,887,273	4,011,968	40.6	3,933,627	98.0
TvAt_72h.3	14,219,218	5,656,869	39.8	5,562,212	98.3
TvAt_96h.1	11,747,581	4,949,453	42.1	4,851,428	98.0
TvAt_96h.2	5,848,710	2,512,642	43.0	2,464,191	98.1
TvAt_96h.3	12,328,096	4,941,085	40.1	4,855,695	98.3

[a]Percentage of mapped reads to the predicted genes.

[b]Percentage of mapped reads with unique hits to the predicted genes

Table 2. List of most specific GO terms enriched in the genes belonging to each cluster created by hierarchical clustering.

Cluster	#Genes	GO_Cat[a]	GO_ID	GO_name	% Seqs[b]	FDR[c]
1	130	BP	GO:0005975	carbohydrate metabolic process	18.4	2.0E-03
		MF	GO:0004553	hydrolase activity, hydrolyzing O-glycosyl compounds	22.4	1.1E-05
		MF	GO:0016798	hydrolase activity, acting on glycosyl bonds	22.4	1.1E-05
		MF	GO:0015926	glucosidase activity	10.5	2.0E-03
2	30	BP	GO:0005975	carbohydrate metabolic process	56.5	3.0E-10
		BP	GO:0080171	lytic vacuole organization	8.7	3.4E-02
		BP	GO:0007040	lysosome organization	8.7	3.4E-02
		BP	GO:0007033	vacuole organization	8.7	4.3E-02
		MF	GO:0001871	pattern binding	39.1	1.5E-14
		MF	GO:0030248	cellulose binding	39.1	1.5E-14
		MF	GO:0030247	polysaccharide binding	39.1	1.5E-14
		MF	GO:0030246	carbohydrate binding	39.1	3.0E-11
		MF	GO:0004553	hydrolase activity, hydrolyzing O-glycosyl compounds	56.5	2.0E-10
		MF	GO:0016798	hydrolase activity, acting on glycosyl bonds	56.5	2.6E-10
		MF	GO:0004348	glucosylceramidase activity	8.7	3.4E-02
		CC	GO:0005576	extracellular region	39.1	1.5E-10
		CC	GO:0005764	lysosome	8.7	3.4E-02
		CC	GO:0000323	lytic vacuole	8.7	4.3E-02
3	81	No enriched GO terms were found				
4	75	No enriched GO terms were found				
5	203	BP	GO:0005975	carbohydrate metabolic process	13.0	2.7E-02
		MF	GO:0003824	catalytic activity	86.1	3.5E-04

		MF	GO:0016491	oxidoreductase activity	35.7	2.2E-03
		MF	GO:0018734	butyrolactone hydrolase activity	3.5	1.8E-02
		MF	GO:0004497	monooxygenase activity	11.3	1.8E-02
		MF	GO:0018733	3,4-dihydrocoumarin hydrolase activity	3.5	1.8E-02
		MF	GO:0018732	sulfolactone hydrolase activity	3.5	1.8E-02
		MF	GO:0018731	1-oxa-2-oxocycloheptane lactonase activity	3.5	1.8E-02
		MF	GO:0046906	tetrapyrrole binding	10.4	2.2E-02
		MF	GO:0020037	heme binding	10.4	2.2E-02
6	53	No enriched GO terms were found				
7	119	BP	GO:0006825	copper ion transport	4.3	1.2E-02
		MF	GO:0000293	ferric-chelate reductase activity	8.6	1.0E-06
		MF	GO:0050660	flavin adenine dinucleotide binding	12.9	2.4E-03
		MF	GO:0005506	iron ion binding	14.3	4.2E-03
		MF	GO:0005375	copper ion transmembrane transporter activity	4.3	1.8E-02
		CC	GO:0016021	integral component of membrane	32.9	5.7E-06

[a] Gene Ontology categories: BP, Biological process; MF, Molecular function; CC, Cellular component.

[b] Percentage of genes belonging to each GO term of the test set.

[c] FDR < 0.05.

Figure Legends

Fig. 1. Transcriptional response of *T. virens* to *Arabidopsis* seedlings. A, Differential expression of *T. virens* genes, during its interaction with *A. thaliana* vs *T. virens* control at 48, 72 and 96 h of co-culture. Differentially expressed genes with an FDR ≤ 0.05. **B,** Venn diagram showing the distribution of induced and repressed genes at 48, 72 and 96 h of interaction. **C**, Hierarchical clustering of the differential gene expression profiles. The dendrogram indicates the relationship between gene expression profiles using the hclust package in R (v3.5.1). Left column colors indicate the clusters created of genes with similar expression patterns, the number of each cluster is indicated. The color key shows the $\log_2$ of fold change (FC) values colors red and blue indicate the up- and downregulated genes using an FDR ≤ 0.05 and $\log_2$FC > 1.

Fig. 2. Validation of RNA-seq by RT-qPCR. *T. virens* was co-cultured with fifteen-day-old *Arabidopsis* seedlings and mycelium was collected at 48,72 and 96 h of co-culture. *T. virens* growing alone in MS medium was included as control. The expression levels of: **A,** putative serine threonine proteine kinase, *kin* (TRIVIDRAFT_58043). **B,** putative heat shock protein, *hsp23* (TRIVIDRAFT_215292). **C,** putative glycoside hydrolase family 18, *gh18* (TRIVIDRAFT_194859). **D,** putative glycoside hydrolase family 7, *gh7* (TRIVIDRAFT_90504). **E,** putative glycosyltransferase family 4 protein *gt4* (TRIVIDRAFT_83336). **F,** putative oxidoreductase FAD/NAD(P)-binding, *oxrdtase* (TRIVIDRAFT_57247). **G,** putative Glutathione-S-transferase, *gst-2* (TRIVIDRAFT_227149). **H,** putative aquaporin, *aqp* (TRIVIDRAFT_6760). **I,** putative 3-hydroxyacyl-CoA dehydrogenase, NAD binding, *3hcd* (TRIVIDRAFT_46955). **J,** putative histone methyltransferase [HMKT], *set* (TRIVIDRAFT_77874). **K,** *ipa-1* (Increased Protection of *Arabidopsis*-1), putative chromatin

remodeler/helicase-related protein (TRIVIDRAFT_113458). **L,** *tbrg-1 (Trichoderma Big Ras-GTPase-1)* (TRIVIDRAFT_70852). **M,** putative Glutathione-S-transferase, *gst-1* (TRIVIDRAFT_34822). **N,** putative glutamine amidotransferase, *pfp-1* glutamine amidotransferase (TRIVIDRAFT_46295). **O,** putative hydrophobin, *TvHyd1* (TRIVIDRAFT_143417). **P,** putative glutamine amidotransferase, *pfp-2* (TRIVIDRAFT_69268). **Q,** putative uptake transporter, *slac-1* (TRIVIDRAFT_158830). **R,** putative ferric reductase-like transmembrane component, *nox* (TRIVIDRAFT_69153). **S,** putative binding protein to unknown toxic compounds, *rta1* (TRIVIDRAFT_59885), were analyzed by RT-qPCR. Results are presented as fold-change in comparison to the fungi growing without *Arabidopsis*. *tef-1* was utilized as control to standardizes the expression level of the genes tested by means of the $2^{-\Delta\Delta Ct}$ method. The RNA-Seq results were validated with one the biological replicates of the transcriptome.

Fig. 3. IPA-1 protein belongs to a new subfamily of the SNF2 of chromatin remodelers/helicase family-related proteins. A, Diagram of domain structure for representative Snf2 family members from *Saccharomyces cerevisiae* and IPA-1 from *T. virens*. Them all share most of all the functional domains of Snf2, including HepA, PLN03142, SNF2_N and DEXH or DEXHc. In addition, Snf2 bears a QL (in blue), which has been shown to be involved in protein-protein interactions and a Bromo (light green) domains, which are involved in recognition of acetylated residues, which results in a re-positioning of the nucleosome and facilitates or represses the binding of gene-specific transcription factors. Rad5 also contains a HIRAN (HIR) domain (light pink) that has been predicted that this protein functions as a DNA-binding domain that probably recognizes features associated with damaged DNA or stalled replication forks. Rad16

bears an Rad18 domain, which is a ring finger ubiquitin ligase related domain. In additions to the shared domains, IPA-1 bears a SF2_C_SNF domain (orange), which putatively participates in RNA and DNA unwinding. The number of amino acids (AA) for each domain and protein is indicated in the figure. **B,** Phylogenetic tree of IPA-1 with members of the subfamilies of the SNF2 family of chromatin remodelers/helicase family-related proteins from *S. cerevisiae*, including Rad16, Mot1, Rad54, Rad5, Rad16, Uls1, Fun30, Chd1, Snf2, Irc5, Swr1, Ino80 and Isw2 and their relatives from *Neurospora crassa* and *T. virens*. The evolutionary history was inferred using the neighbor-joining method. The bootstrap consensus tree inferred from 1500 replicates was chosen to represent the evolutionary history of the taxa analyzed. The evolutionary distances were computed using the Poisson correction method and are in the units of the number of amino acid substitutions per site. Evolutionary analyses were conducted in MEGAX. Tv, *T. virens*; Nc, *N. crassa*.

Fig. 4. Mycelial free culture filtrates (MFCF) of Δ*ipa-1-23* showed diminished inhibition of *R. solani* growth. The WT and Δ*ipa-1-23* strains were grown in PDB media for 4 days and MFCF were used to amend PDA plates at 40%. **A,** Representative pictures of *R. solani* radial growth at 24, 48, 72 and 96 h on MFCF WT and Δ*ipa-1-23* strains. **B,** % of growth inhibition of *R. solani* at 24, 48, 72 and 96 h in PDA plates amended with MFCF WT and Δ*ipa-1-23* strains. Data from B show the mean ± SD of three independent experiments (3 plates for treatment). Asterisks show significant difference (independent Student's t-test, $P < 0.001$**). *Significant difference between Control vs. WT or Δ*ipa-1-23*. **Significant difference between WT vs. Δ*ipa-1-23*.

Fig. 5. Deletion of *ipa-1* resulted in an enhanced plant protection against *P. syringae*. Ten-day-old *Arabidopsis* plants grown on MS medium were root-inoculated with the WT, Δ*ipa-1-23* and Δ*ipa-1-24*, the expression levels of **A,** *PR-1a* or **B,** *PDF1.2* were analyzed by RT-qPCR at 48, 72 and 96 hpi. RT-qPCR results are presented as fold-change compared to *Arabidopsis* growing without the fungi. *Arabidopsis ACT2* gene was utilized as control to standardize the expression of *PR-1a* and *PDF1.2* by means of the $2^{-\Delta\Delta Ct}$ method. Ten-day-old *Arabidopsis* seedlings grown in soil and inoculated with the WT or Δ*ipa-1*, and 2 weeks later leaves were infected with **C,** *B. cinerea* or inoculating buffer as control. **D**, Lesion sizes of infected plants with *B. cinerea* were determined using ImageJ at 6 dpi**. E**, Colony forming units of *Pst* DC3000 at 0 and 3 dpi in leaves of treated and untreated plants with WT or Δ*ipa-1*. Data from (A-B) show the mean ± SD of at least 5 plates with 7 plants. The trial was repeated twice with comparable results. Asterisks show significant difference (independent Student's t-test, $P < 0.05$). * significant difference between Control vs. WT, Δ*ipa-1-23* or Δ*ipa-1-24*. **Significant difference between WT vs. Δ*ipa-1-23* or Δ*ipa-1-24*. Data from (D-E) show the mean ± SD of at least 12 leaves. The trial was repeated twice with comparable results. Asterisks show significant difference (independent t-test, $*P < 0.05$).

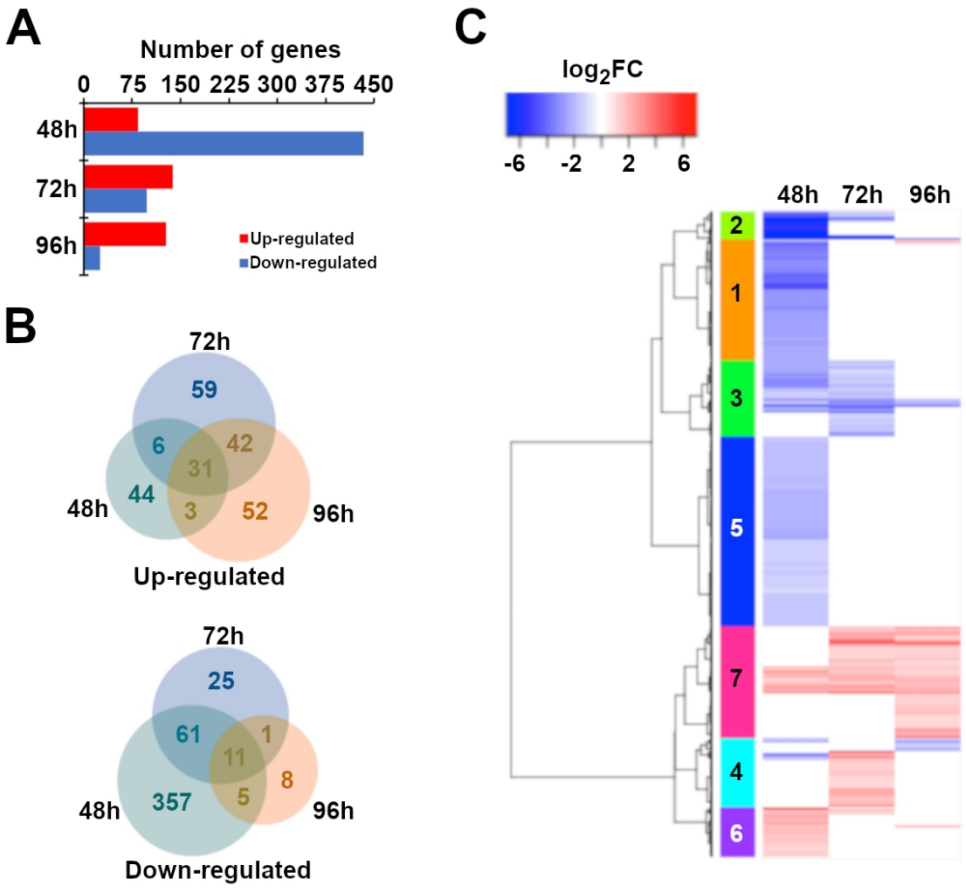

Fig. 1. Transcriptional response of *T. virens* to *Arabidopsis* seedlings. A, Differential expression of *T. virens* genes, during its interaction with *A. thaliana* vs *T. virens* control at 48, 72 and 96 h of co-culture. Differentially expressed genes with an FDR ≤ 0.05. B, Venn diagram showing the distribution of induced and repressed genes at 48, 72 and 96 h of interaction. C, Hierarchical clustering of the differential gene expression profiles. The dendrogram indicates the relationship between gene expression profiles using the hclust package in R (v3.5.1). Left column colors indicate the clusters created of genes with similar expression patterns, the number of each cluster is indicated. The color key shows the $\log_2$ of fold change (FC) values colors red and blue indicate the up- and down-regulated genes using an FDR ≤ 0.05 and $\log_2$ FC > 1.

99x92mm (300 x 300 DPI)

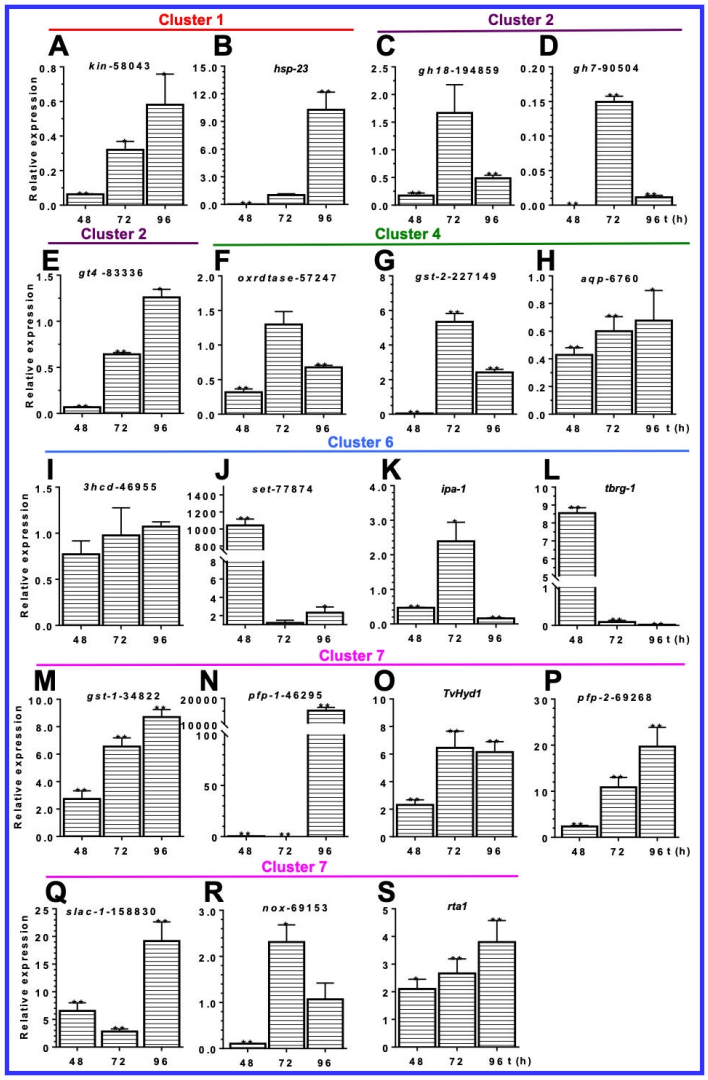

Fig. 2. Validation of RNA-seq by RT-qPCR. *T. virens* was co-cultured with fifteen-day-old *Arabidopsis* seedlings and mycelium was collected at 48,72 and 96 h of co-culture. *T. virens* growing alone in MS medium was included as control. The expression levels of: A, putative serine threonine proteine kinase, *kin* (TRIVIDRAFT_58043). B, putative heat shock protein, *hsp23* (TRIVIDRAFT_215292). C, putative glycoside hydrolase family 18, *gh18* (TRIVIDRAFT_194859). D, putative glycoside hydrolase family 7, *gh7* (TRIVIDRAFT_90504). E, putative glycosyltransferase family 4 protein *gt4* (TRIVIDRAFT_83336). F, putative oxidoreductase FAD/NAD(P)-binding, *oxrdtase* (TRIVIDRAFT_57247). G, putative Glutathione-S-transferase, *gst-2* (TRIVIDRAFT_227149). H, putative aquaporin, *aqp* (TRIVIDRAFT_6760). I, putative 3-hydroxyacyl-CoA dehydrogenase, NAD binding, *3hcd* (TRIVIDRAFT_46955). J, putative histone methyltransferase [HMKT], *set* (TRIVIDRAFT_77874). K, *ipa-1* (Increased Protection of Arabidopsis-1), putative chromatin remodeler/helicase-related protein (TRIVIDRAFT_113458). L, *tbrg-1* (Trichoderma Big Ras-GTPase-1) (TRIVIDRAFT_70852). M, putative Glutathione-S-transferase, *gst-1* (TRIVIDRAFT_34822). N, putative glutamine amidotransferase, *pfp-1* glutamine amidotransferase (TRIVIDRAFT_46295). O, putative hydrophobin, *TvHyd1* (TRIVIDRAFT_143417). P, putative glutamine amidotransferase, *pfp-2*

(TRIVIDRAFT_69268). Q, putative uptake transporter, *slac-1* (TRIVIDRAFT_158830). R, putative ferric reductase-like transmembrane component, *nox* (TRIVIDRAFT_69153). S, putative binding protein to unknown toxic compounds, *rta1* (TRIVIDRAFT_59885), were analyzed by RT-qPCR. Results are presented as fold-change in comparison to the fungi growing without Arabidopsis. *tef-1* was utilized as control to standardizes the expression level of the genes tested by means of the $2^{-\Delta\Delta Ct}$ method. The RNA-Seq results were validated with one the biological replicates of the transcriptome.

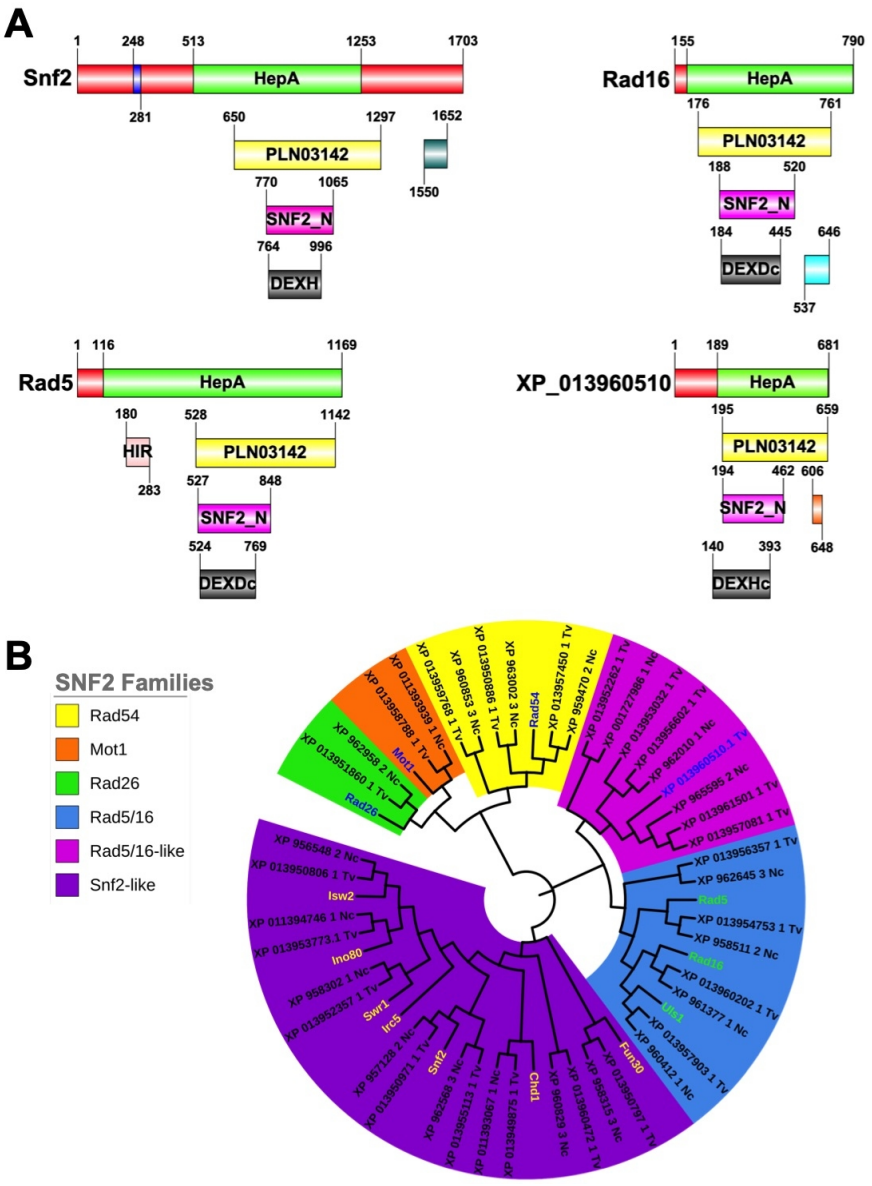

Fig. 3. IPA-1 protein belongs to a new subfamily of the SNF2 of chromatin remodelers/helicase family-related proteins. A, Diagram of domain structure for representative Snf2 family members from *Saccharomyces cerevisiae* and IPA-1 from *T. virens*. Them all share most of all the functional domains of Snf2, including HepA, PLN03142, SNF2_N and DEXH or DEXHc. In addition, Snf2 bears a QL (in blue), which has been shown to be involved in protein-protein interactions and a Bromo (light green) domains, which are involved in recognition of acetylated residues, which results in a re-positioning of the nucleosome and facilitates or represses the binding of gene-specific transcription factors. Rad5 also contains a HIRAN (HIR) domain (light pink) that has been predicted that this protein functions as a DNA-binding domain that probably recognizes features associated with damaged DNA or stalled replication forks. Rad16 bears an Rad18 domain, which is a ring finger ubiquitin ligase related domain. In additions to the shared domains, IPA-1 bears a SF2_C_SNF domain (orange), which putatively participates in RNA and DNA unwinding. The number of amino acids (AA) for each domain and protein is indicated in the figure. B, Phylogenetic tree of IPA-1 with members of the subfamilies of the SNF2 family of chromatin remodelers/helicase family-related proteins from S. cerevisiae, including Rad16, Mot1, Rad54, Rad5, Rad16, Uls1, Fun30, Chd1, Snf2, Irc5,

Swr1, Ino80 and Isw2 and their relatives from *Neurospora crassa* and *T. virens*. The evolutionary history was inferred using the neighbor-joining method. The bootstrap consensus tree inferred from 1500 replicates was chosen to represent the evolutionary history of the taxa analyzed. The evolutionary distances were computed using the Poisson correction method and are in the units of the number of amino acid substitutions per site. Evolutionary analyses were conducted in MEGAX. Tv, *T. virens*; Nc, *N. crassa*.

190x254mm (150 x 150 DPI)

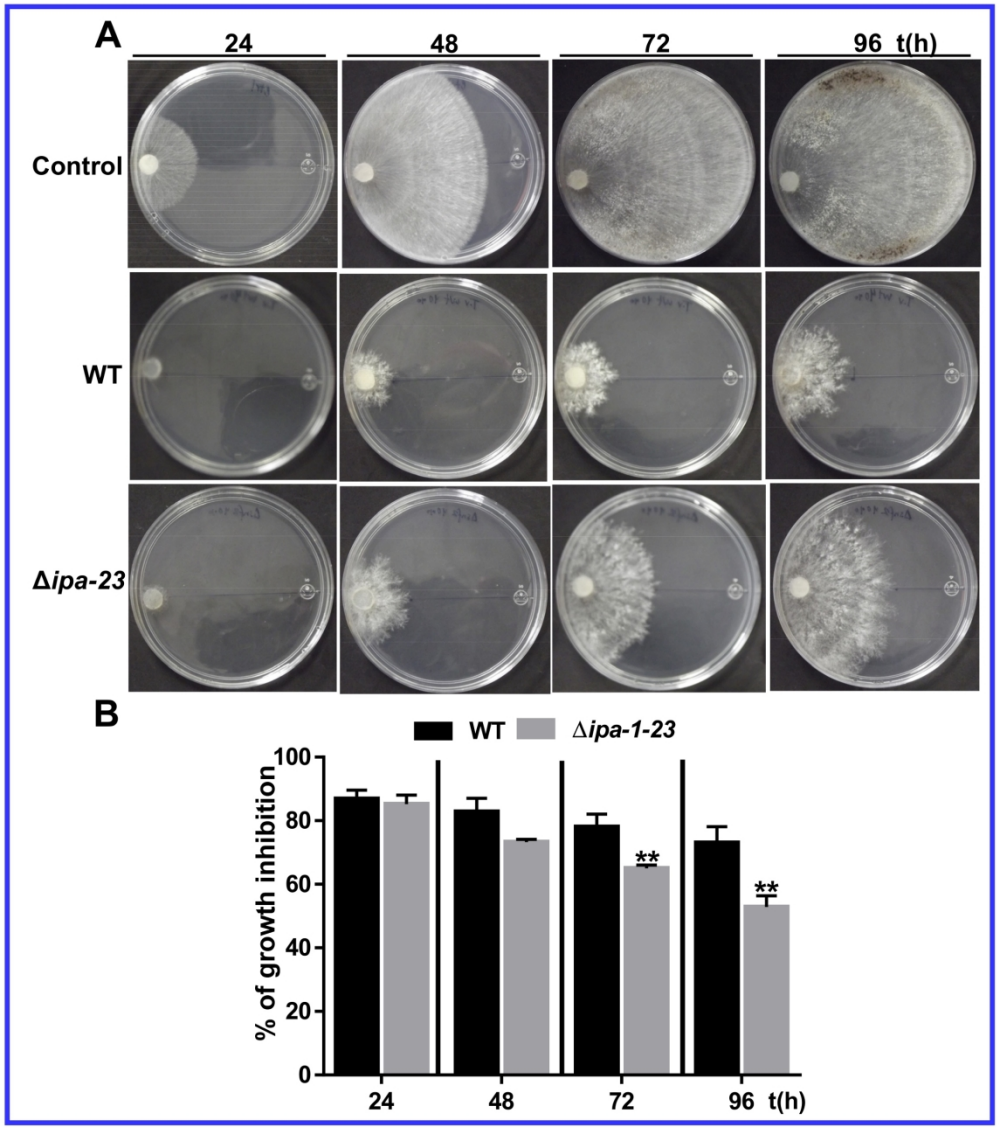

Fig. 4. Mycelial free culture Filtrates (MFCF) of Δ*ipa-1-23* showed diminished inhibition of *R. solani* growth. The WT and Δ*ipa-1-23* strains were grown in PDB media for 4 days and MFCF were used to amend PDA plates at 40%. A, Representative pictures of *R. solani* radial growth at 24, 48, 72 and 96 h on MFCF WT and Δ*ipa-1-23* strains. B, % of growth inhibition of *R. solani* at 24, 48, 72 and 96 h in PDA plates amended with MFCF WT and Δ*ipa-1-23* strains. Data from B show the mean ± SD of three independent experiments (3 plates for treatment). Asterisks show significant difference (independent Student's t-test, $P < 0.001$**). *Significant difference between Control vs. WT or Δ*ipa-1-23*. **Significant difference between WT vs. Δ*ipa-1-23*.

63x72mm (900 x 900 DPI)

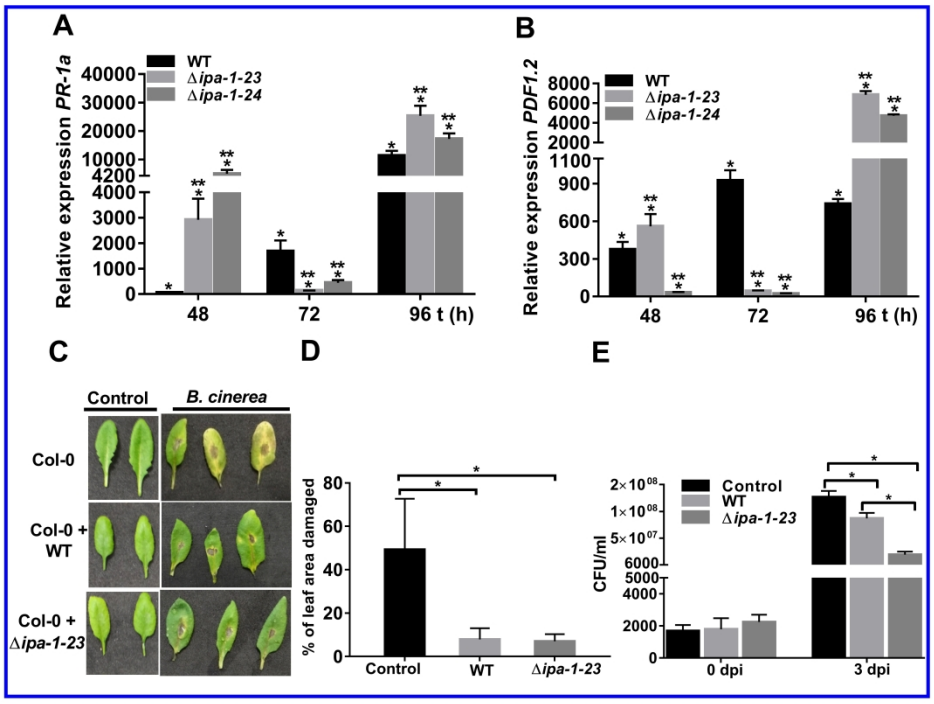

Fig. 5. Deletion of *ipa-1* resulted in an enhanced plant protection against *P. syringae*. Ten-day-old *Arabidopsis* plants grown on MS medium were root-inoculated with the WT, Δ*ipa-1-23* and Δ*ipa-1-24*, the expression levels of A, *PR-1a* or B, *PDF1.2* were analyzed by RT-qPCR at 48, 72 and 96 hpi. RT-qPCR results are presented as fold-change compared to *Arabidopsis* growing without the fungi. Arabidopsis *ACT2* gene was utilized as control to standardize the expression of *PR-1a* and *PDF1.2* by means of the 2-ΔΔCt method. Ten-day-old *Arabidopsis* seedlings grown in soil and inoculated with the WT or Δ*ipa-1*, and 2 weeks later leaves were infected with C, *B. cinerea* or inoculating buffer as control. D, Lesion sizes of infected plants with *B. cinerea* were determined using ImageJ at 6 dpi. E, Colony forming units of *Pst* DC3000 at 0 and 3 dpi in leaves of treated and untreated plants with WT or Δ*ipa-1.* Data from (A-B) show the mean ± SD of at least 5 plates with 7 plants. The trial was repeated twice with comparable results. Asterisks show significant difference (independent Student's t-test, $P < 0.05$). * significant difference between Control vs. WT, Δ*ipa-1-23* or Δ*ipa-1-24*. **Significant difference between WT vs. Δ*ipa-1-23* or Δ*ipa-1-24*. Data from (D-E) show the mean ± SD of at least 12 leaves. The trial was repeated twice with comparable results. Asterisks show significant difference (independent t-test, *$P < 0.05$).

219x157mm (600 x 600 DPI)

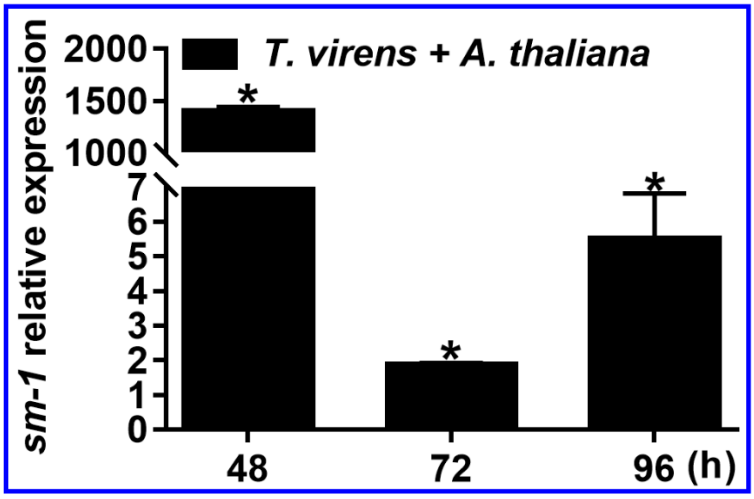

Supplementary Fig. S1. The mRNA levels of *sm-1* were induced in *Trichoderma* in the presence of *Arabidopsis* Col-0 seedling. 15-day-old *Arabidopsis* Col-0 seedlings were root-inoculated with *T. virens*-WT actively growing mycelium. *Trichoderma* growing in MS medium alone was included as control. The mycelium was collected at 48, 72 and 96 of co-culture. The expression levels of *sm-1* were analyzed by RT-qPCR. The graphs show the mean expression levels ± SD. RT-qPCR results are reported as fold-change compared to the fungi growing without *Arabidopsis*. *tef-1* was used as control gene to normalize the expression of *hda-2* using the $2^{-\Delta\Delta Ct}$ method.

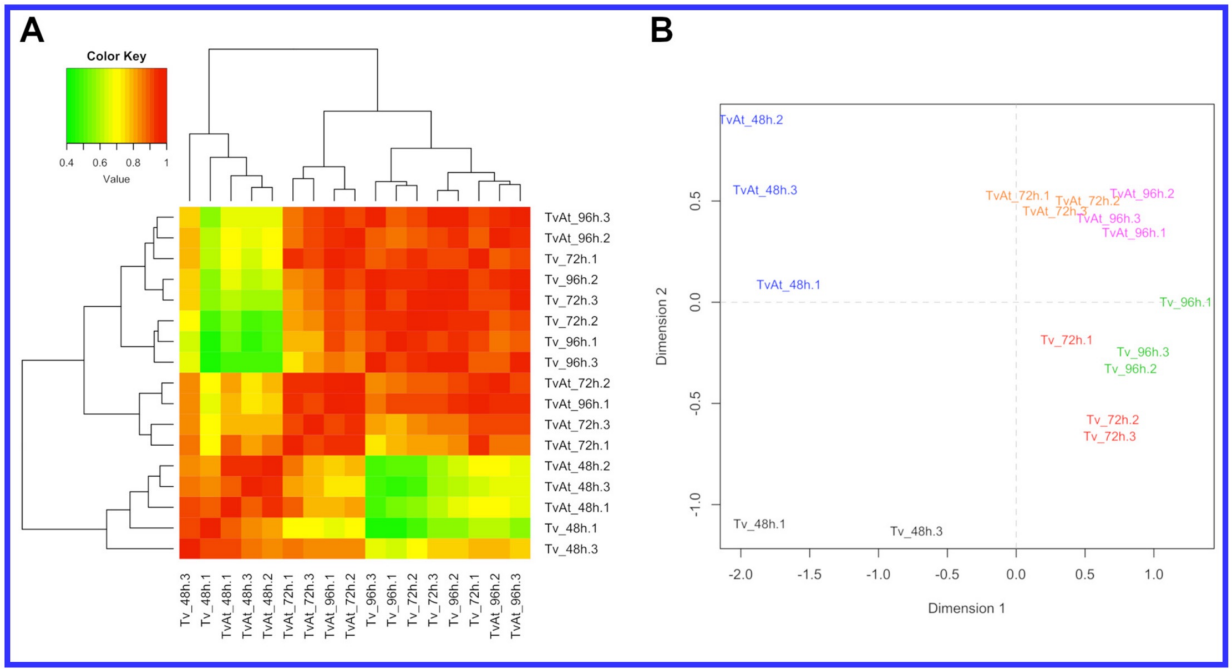

Supplementary Fig. S2. Overview of gene expression profiles of biological replicates. A, Heat-map of Pearson's correlation of the transcript expression levels of control and treated samples at 48, 72 and 96 co-culture. Color key indicates the Pearson's correlation values from 0.4 to 1, Red – highly correlated samples, green – low correlation. **B,** Multidimensional scaling plot showing the distances of the biological coefficient of variation between each pair of samples. Tv (*T. virens* control); TvAt, (Interaction *T. virens*-*A. thaliana*). The biological replication number is indicated after the dot. Raw count data were normalized using the edgeR (Robinson et al. 2010).

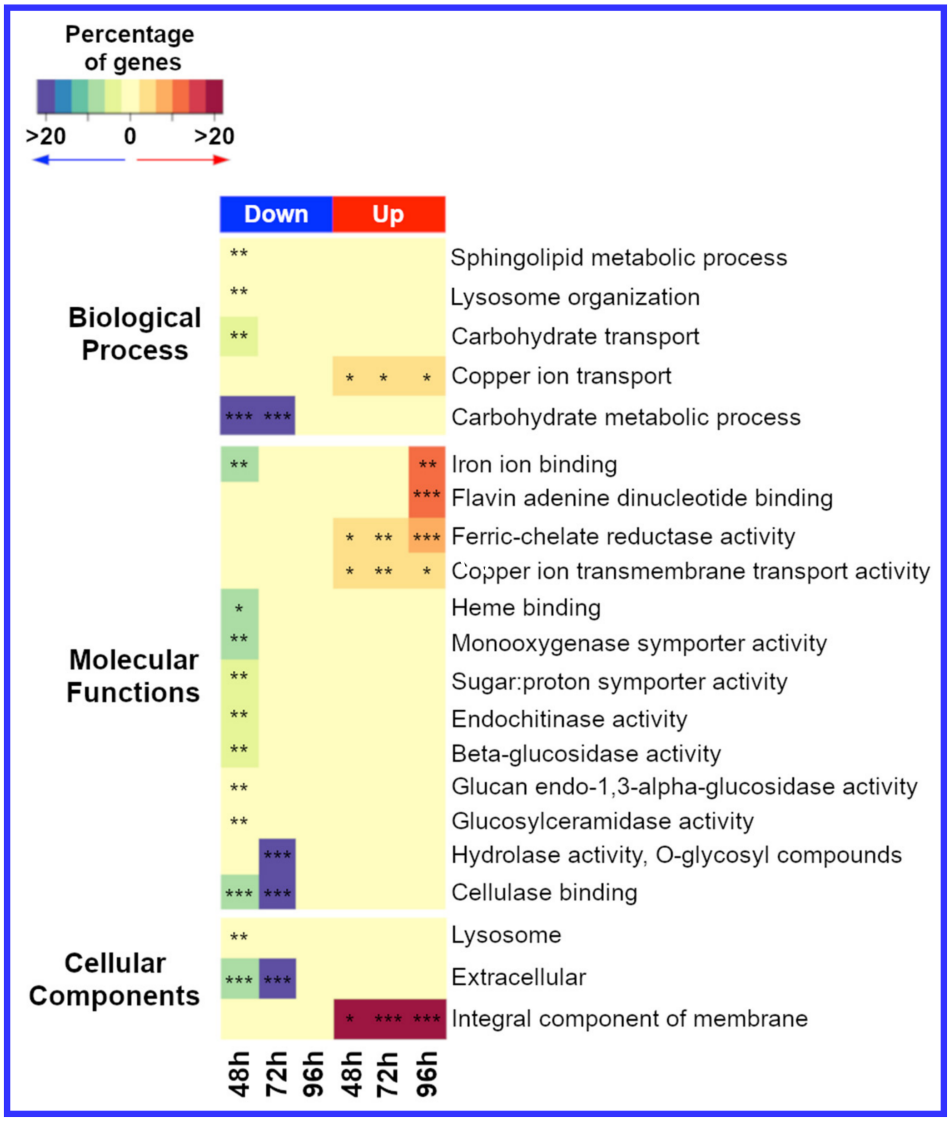

Supplementary Fig. S3. Heatmap of gene ontology enrichment of *T. virens* up- and down-regulated genes during its interaction with *Arabidopsis* seedlings at 48, 72 and 96 h of co-culture. Each column contains the up- (top bar red) and down-regulated GO terms (top bar blue). Only the most specific GO terms are shown (FDR< 0.05). Color scale shows the percentage of genes, belonging to each up-regulated (arrow red) and down-regulated GO terms. Asterisks represent the statistical significance of enrichment (*FDR<0.05, **FDR<0.01, ***FDR<0.001).

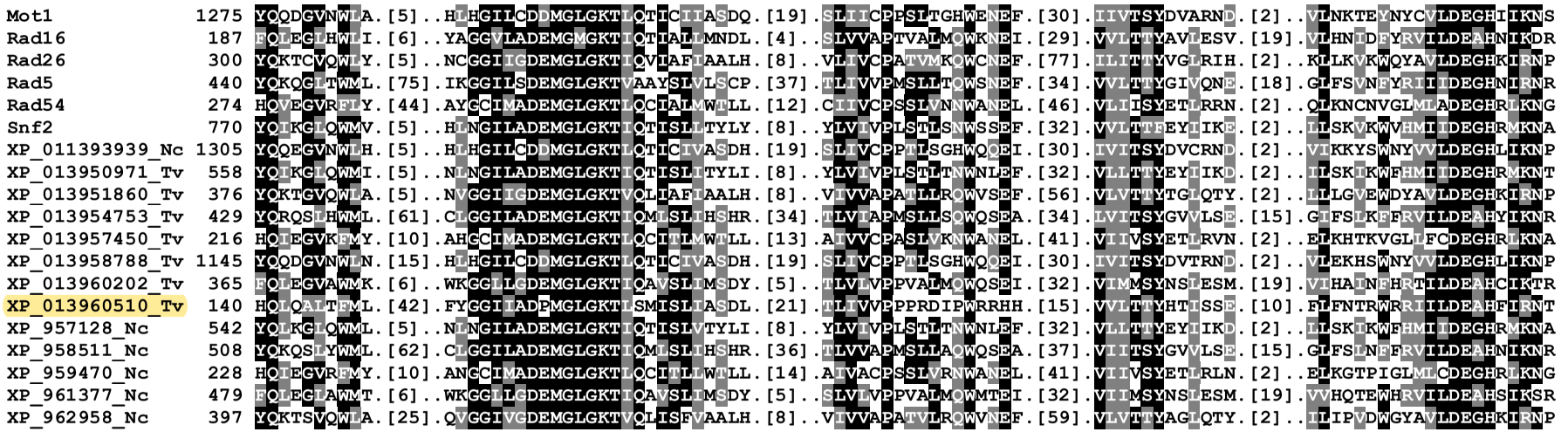
Mot1 1275 YQQDGVNWLA.[5]..HLHGILCDDMGLGKTLQTICIIASDQ.[19].SLIICPPSLTGHWENEF.[30].IIVTSYDVARND.[2]..VLNKTEYNYCVLDEGHIIKNS
Rad16 187 FQLEGLHWLI.[6]..YAGGVLADEMGMGKTIQTIALLMNDL.[4]..SLVVAPTVALMQWKNEI.[29].VVLTTYAVLESV.[19].VLHNIDFYRVILDEAHNIKDR
Rad26 300 YQKTCVQWLY.[5]..NCGGIIGDEMGLGKTIQVIAFLAALH.[8]..VLIVCPATVMKQWCNEF.[77].ILITTYVGLRIH.[2]..KLLKVKWQYAVLDEGHKIRNP
Rad5 440 YQKQGLTWML.[75].IKGGILSDEMGLGKTVAAYSLVLSCP.[37].TLIVVPMSLLTQWSNEF.[34].VVLTTYGIVQNE.[18].GLFSVNFYRIIIDEGHNIRNR
Rad54 274 HQVEGVRFLY.[44].AYGCIMADEMGLGKTLQCTALVWLLL.[12].CIIVCPSSLVNNWANEL.[46].VLIISYETLRRN.[2]..QLKNCNVGLMLADEGHRLKNG
Snf2 770 YQIKGLQWMV.[5]..HLNGILADEMGLGKTIQTISLLTYLY.[8]..YLVIVPLSTLSNWSSEF.[32].VVLTTFEYIIKE.[2]..LLSKVKWVHMIIDEGHRMKNA
XP_011393939_Nc 1305 YQQEGVNWLH.[5]..HLHGILCDDMGLGKTLQTICIVASDH.[19].SLIVCPPTLSGHWQQEI.[30].IVITSYDVCRND.[2]..VIKKYSWNYVVLDEGHLIKNP
XP_013950971_Tv 558 YQIKGLQWMI.[5]..NLNGILADEMGLGKTIQTISLITYLI.[8]..YLVIVPLSTLTNWNLEF.[32].VLLTTYEYIIKD.[2]..ILSKIKWFHMIIDEGHRMKNT
XP_013951860_Tv 376 YQKTGVQWLA.[5]..NVGGIIGDEMGLGKTVQLIAFLAALH.[8]..VIVVAPATLLRQWVSEF.[56].VLVTTYTGLQTY.[2]..LLLGVEWDYAVLDEGHKIRNP
XP_013954753_Tv 429 YQRQSLHWML.[61].CLGGILADEMGLGKTIQMLSLIHSHR.[34].TLVIAPMSLLSQWQSEA.[34].LVITSYGVVLSE.[15].GIFSLKFFRVILDEAHYIKNR
XP_013957450_Tv 216 HQIEGVKFMY.[10].AHGCIMADEMGLGKTLQCITLVWLLL.[13].AIVVCPASLVKNWANEL.[41].VIIVSYETLRVN.[2]..ELKHTKVGLLFCDEGHRLKNA
XP_013958788_Tv 1145 YQQDGVNWLN.[15].HLHGILCDDMGLGKTLQTICIVASDH.[19].SLIVCPPTLSGHWQQEI.[30].IVITSYDVTRND.[2]..VLEKHSWNYVVLDEGHLIKNP
XP_013960202_Tv 365 FQLEGVAWMK.[6]..WKGGLLGDEMGLGKTIQAVSLIMSDY.[5]..TLVLVPPVALMQWQSEI.[32].VIMMSYNSLESM.[19].VIHAINPHRTILDEAHCIKTR
XP_013960510_Tv 140 HQLQAITFML.[42].FYGGIIADPMGLGKTLSMISLIASDL.[21].TLIVVPPPRDIPWRRHH.[15].VVLTTYHTISSE.[10].FLFNTRWRRIILDEAHFIRNT
XP_957128_Nc 542 YQLKGLQWML.[5]..NLNGILADEMGLGKTIQTISLVTYLI.[8]..YLVIVPLSTLTNWNLEF.[32].VLLTTYEYIIKD.[2]..LLSKIKWFHMIIDEGHRMKNA
XP_958511_Nc 508 YQKQSLYWML.[62].CLGGILADEMGLGKTIQMLSLIHSHR.[36].TLVVAPMSLLAQWQSEA.[37].VIITSYGVVLSE.[15].GLFSLNFFRVILDEAHNIKNR
XP_959470_Nc 228 HQIEGVRFMY.[10].ANGCIMADEMGLGKTLQCITLLWLLL.[14].AIVACPSSLVRNWANEL.[41].VIIVSYETLRLN.[2]..ELKGTPIGLMLCDEGHRLKNG
XP_961377_Nc 479 FQLEGLAWMT.[6]..WKGGLLGDEMGLGKTIQAVSLIMSDY.[5]..SLVLVPPVALMQWMTEI.[32].VIIMSYNSLESM.[19].VVHQTEWHRVILDEAHSIKSR
XP_962958_Nc 397 YQKTSVQWLA.[25].QVGGIVGDEMGLGKTVQLISFVAALH.[8]..VIVVAPATVLRQWVNEF.[59].VLVTTYAGLQTY.[2]..ILIPVDWGYAVLDEGHKIRNP

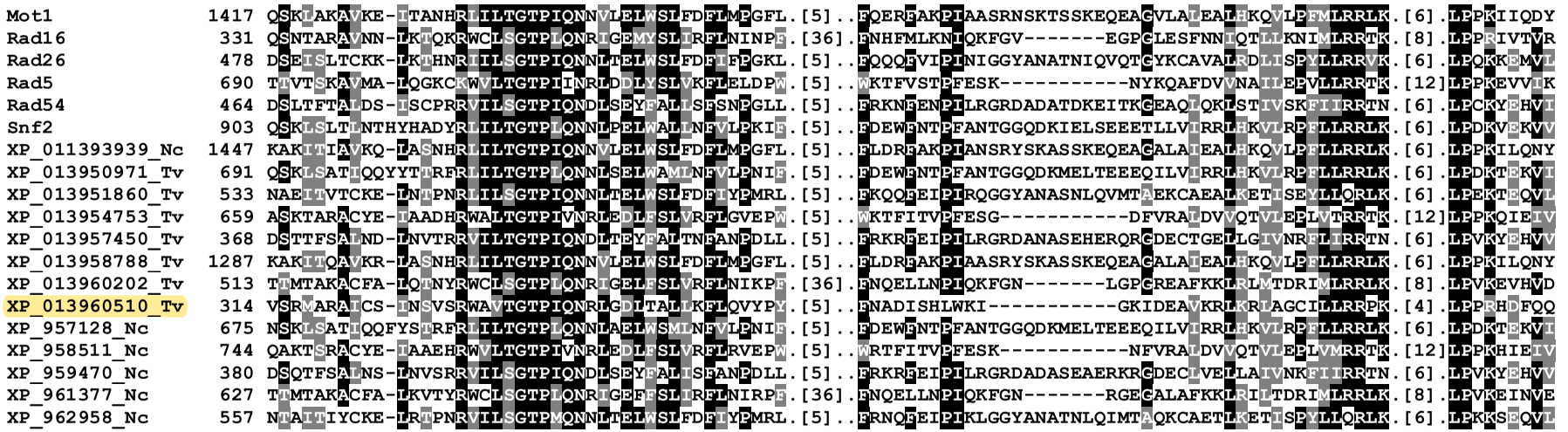
Mot1 1417 QSKLAKAVKE-ITANHRLILTGTPIQNNVLELWSLFDFTMPGFL.[5]..FQERFAKPIAASRNSKTSSKEQEAGVLALEALHKQVLPFMLRRLK.[6].LPPKIIQDY
Rad16 331 QSNTARAVNN-LKTQKRWCLSGTPLQNRIGEMYSLIRFTNINPF.[36].FNHFMLKNIQKFGV-------EGPGLESFNNIQTLLKNIMLRRTK.[8].LPPRIVTVR
Rad26 478 DSEISLTCKK-LKTHNRIILSGTPIQNNLTELWSLFDFTFPGKL.[5]..FQQQFVIPINIGGYANATNIQVQTGYKCAVALRDLISPYLLRRVK.[6].LPQKKEMVL
Rad5 690 TTVTSKAVMA-LQGKCKWVLTGTPIINRLDDLYSLVKFTELDPW.[5]..WKTFVSTPFESK----------NYKQAFDVVNAILEPVLLRRTK.[12]LPPKEVVIK
Rad54 464 DSLTFTALDS-ISCPRRVILSGTPIQNDLSEYFALISFSNPGLL.[5]..FRKNFENPILRGRDADATDKEITKGEAQLQKLSTIVSKFIIRRTN.[6].LPCKYEHVI
Snf2 903 QSKLSLTLNTHYHADYRLILTGTPLQNNLPELWALLNFVLPKIF.[5]..FDEWFNTPFANTGGQDKIELSEEETLLVIRRLHKVLRPFLLRRLK.[6].LPDKVEKVV
XP_011393939_Nc 1447 KAKITIAVKQ-LASNHRLILTGTPIQNNVLELWSLFDFLMPGFL.[5]..FLDRFAKPIANSRYSKASSKEQEAGALAIEALHKQVLPFLLRRLK.[6].LPPKILQNY
XP_013950971_Tv 691 QSKLSATLQQYYTTRFRLILTGTPLQNNLSELWAMLNFVLPNIF.[5]..FDEWFNTPFANTGGQDKMELTEEEQILVIRRLHKVLRPFLLRRLK.[6].LPDKTEKVI
XP_013951860_Tv 533 NAEITVTCKE-LNTPNRLILSGTPIQNNLTELWSLFDFIYPMRL.[5]..FKQQFEIPIRQGGYANASNLQVMTAEKCAEALKETISEYLLQRLK.[6].LPEKTEQVL
XP_013954753_Tv 659 ASKTARACYE-LAADHRWALTGTPIVNRLEDLFSLVRFTGVEPW.[5]..WKTFITVPFESG----------DFVRALDVVQTVLEPLVTRRTK.[12]LPPKQIEIV
XP_013957450_Tv 368 DSTTFSALND-LNVTRRVILTGTPIQNDLTEYFALTNFANPDLL.[5]..FRKRFEIPILRGRDANASEHERQRGDECTGELLGIVNRFLIRRTN.[6].LPVKYEHVV
XP_013958788_Tv 1287 KAKITQAVKR-LASNHRLILTGTPIQNNVLELWSLFDFLMPGFL.[5]..FLDRFAKPIAASRYSKASSKEQEAGALAIEALHKQVLPFLLRRLK.[6].LPPKILQNY
XP_013960202_Tv 513 TLMTAKACFA-LQTNYRWCLSGTPLQNRIGELFSLVRFLNIKPF.[36].FNQELLNPIQKFGN-------LGPGREAFKKLRLMTDRIMLRRLK.[8].LPVKEVHVD
XP_013960510_Tv 314 VSRVARALCS-LNSVSRWAVTGTPIQNRLGDLTALLKFLQVYPY.[5]..FNADISHLWKI----------GKIDEAVKRLKRLAGCILLRRPK.[4].LPPFHDFQQ
XP_957128_Nc 675 NSKLSATLQQFYSTRFRLILTGTPLQNNLAELWSMLNFVLPNIF.[5]..FDEWFNTPFANTGGQDKMELTEEEQILVIRRLHKVLRPFLLRRLK.[6].LPDKTEKVI
XP_958511_Nc 744 QAKTSRACYE-IAAEHRWVLTGTPIVNRLEDLFSLVRFTRVEPW.[5]..WRTFITVPFESK----------NFVRALDVVQTVLEPLVMRRTK.[12]LPPKHIEIV
XP_959470_Nc 380 DSQTFSALNS-LNVSRRVILSGTPIQNDLSEYFALISFANPDLL.[5]..FRKRFEIPILRGRDADASEAERKRGDECLVELLAIVNKFIIRRTN.[6].LPVKYEHVV
XP_961377_Nc 627 TLMTAKACFA-LKVTYRWCLSGTPLQNRIGEFFSLIRFLNIRPF.[36].FNQELLNPIQKFGN-------RGEGALAFKKLRILTDRIMLRRLK.[8].LPVKEINVE
XP_962958_Nc 557 NTAITIYCKE-LRTPNRVILSGTPMQNNLTELWSLFDFIYPMRL.[5]..FRNQFEIPIKLGGYANATNLQIMTAQKCAETLKETISPYLLQRLK.[6].LPKKSEQVL

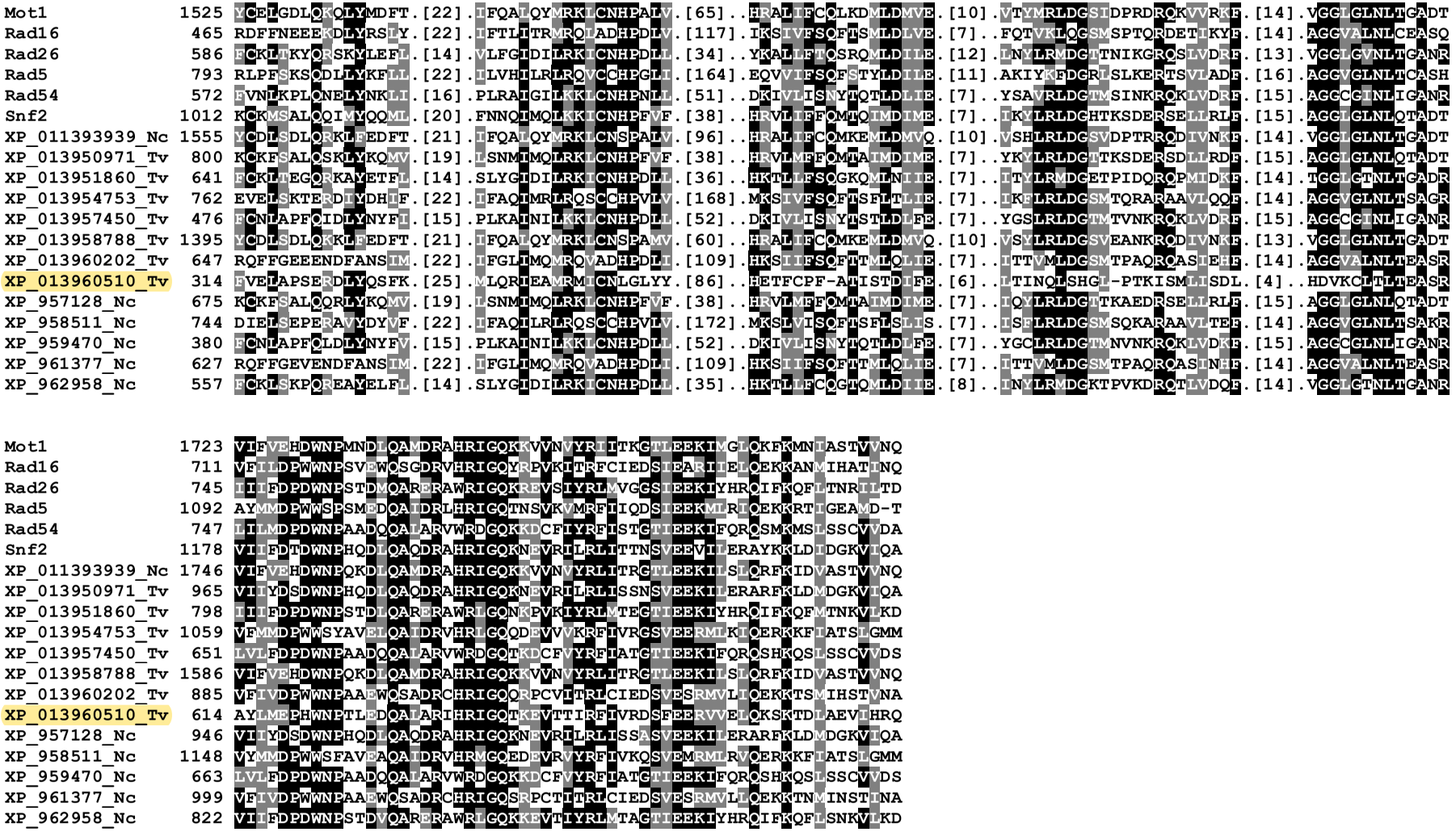
Mot1 1525 YCELGDLQKQLYMDFT.[22].IFQALQYMRKLCNHPALV.[65]..HRALIFCQLKDMLDMVE.[10].VTYMRLDGSIDPRDRQKVVRKF.[14].VGGLGLNLTGADT
Rad16 465 RDFFNEEEKDLYRSLY.[22].IFTLITRMRQLADHPDLV.[117].IKSIVFSQFTSMLDLVE.[7]..FQTVKLQGSMSPTQRDETIKYF.[14].AGGVALNLCEASQ
Rad26 586 FCKLIKYQRSKYLEFL.[14].VLFGIDILRKICNHPDLL.[34]..YKALLFTQSRQMLDILE.[12].LNYLRMDGTTNIKGRQSLVDRF.[13].VGGLGVNLTGANR
Rad5 793 RLPFSKSQDILYKFLL.[22].ILVHILRLRQVCCHPGLI.[164].EQVVIFSQFSTYLDILE.[11].AKIYKFDGRLSLKERTSVLADF.[16].AGGVGLNLTCASH
Rad54 572 EVNLKPLQNELYNKLI.[16].PLRAIGILKKLCNHPNLL.[51]..DKIVLISNYTQTLDLIE.[7]..YSAVRLDGTMSINKRQKLVDRF.[15].AGGCGINLIGANR
Snf2 1012 KCKMSALQQIMYQQML.[20].FNNQIMQLKKICNHPFVF.[38]..HRVLIFFQMTQIMDIME.[7]..IKYLRLDGHTKSDERSELLRLF.[15].AGGLGLNLQTADT
XP_011393939_Nc 1555 YCDLSDLQRKLFEDFT.[21].IFQALQYMRKLCNSPALV.[96]..HRALIFCQMKEMLDMVQ.[10].VSHLRLDGSVDPTRRQDIVNKF.[14].VGGLGLNLTGADT
XP_013950971_Tv 800 KCKFSALQSKLYKQMV.[19].LSNMIMQLRKLCNHPFVF.[38]..HRVLMFFQMTAIMDIME.[7]..YKYLRLDGTTKSDERSDLLRDF.[15].AGGLGLNLQTADT
XP_013951860_Tv 641 FCKLIEGQRKAYETFL.[14].SLYGIDILRKICNHPDLL.[36]..HKTLLFSQGKQMLNIIE.[7]..ITYLRMDGETPIDQRQPMIDKF.[14].TGGLGTNLTGADR
XP_013954753_Tv 762 EVELSKTERDIYDHIF.[22].IFAQIMRLRQSCCHPVLV.[168].MKSIVFSQFTSFLTLIE.[7]..IKFLRLDGSMTQRARAAVLQQF.[14].AGGVGLNLTSAGR
XP_013957450_Tv 476 FCNLAPFQIDLYNYFL.[15].PLKAINILKKLCNHPDLL.[52]..DKIVLISNYTSTLDLFE.[7]..YGSLRLDGTMTVNKRQKLVDRF.[15].AGGCGINLIGANR
XP_013958788_Tv 1395 YCDLSDLQKKLFEDFT.[21].IFQALQYMRKLCNSPAMV.[60]..HRALIFCQMKEMLDMVQ.[10].VSYLRLDGSVEANKRQDIVNKF.[13].VGGLGLNLTGADT
XP_013960202_Tv 647 RQFFGEEENDFANSIM.[22].IFGLIMQMRQVADHPDLI.[109].HKSIIFSQFTTMLQLIE.[7]..ITTVMLDGSMTPAQRQASIEHF.[14].AGGVALNLTEASR
XP_013960510_Tv 314 EVELAPSERDLYQSFK.[25].MLQRIEAMRMICNLGLYY.[86]..HETFCPF-ATISTDIFE.[6]..ITINQLSHGL-PTKISMLISDL.[4]..HDVKCLTLTEASR
XP_957128_Nc 675 KCKFSALQQRLYKQMV.[19].LSNMIMQLRKLCNHPFVF.[38]..HRVLMFFQMTAIMDIME.[7]..IQYLRLDGTTKAEDRSELLRLF.[15].AGGLGLNLQTADT
XP_958511_Nc 744 DIELSEPERAVYDYVF.[22].IFAQILRLRQSCCHPVLV.[172].MKSLVISQFTSFLSLIS.[7]..ISFLRLDGSMSQKARAAVLTEF.[14].AGGVGLNLTSAKR
XP_959470_Nc 380 FCNLAPFQLDLYNYFV.[15].PLKAINILKKLCNHPDLL.[52]..DKIVLISNYTQTLDLFE.[7]..YGCLRLDGTMNVNKRQKLVDKF.[15].AGGCGLNLIGANR
XP_961377_Nc 627 RQFFGEVENDFANSIM.[22].IFGLIMQMRQVADHPDLI.[109].HKSIIFSQFTTMLQLIE.[7]..ITTVMLDGSMTPAQRQASINHF.[14].AGGVALNLTEASR
XP_962958_Nc 557 FCKLSKPQREAYELFL.[14].SLYGIDILRKICNHPDLL.[35]..HKTLLFCQGTQMLDIIE.[8]..INYLRMDGKTPVKDRQTLVDQF.[14].VGGLGTNLTGANR

Mot1 1723 VIFVEHDWNPMNDLQAMDRAHRIGQKKVVNVYRLITKGTLEEKIMGLQKFKMNIASTVVNQ
Rad16 711 VFILDPWWNPSVEWQSGDRVHRIGQYRPVKITRFCIEDSIEARIIELQEKKANMIHATINQ
Rad26 745 IIIFDPDWNPSTDMQARERAWRIGQKREVSIYRLMVGGSIEEKIYHRQIFKQFLTNRILTD
Rad5 1092 AYMMDPWWSPSMEDQAIDRLHRIGQTNSVKVMRFIIQDSIEEKMLRIQEKKRTIGEAMD-T
Rad54 747 LILMDPDWNPAADQQALARVWRDGQKKDCFIYRFISTGTIEEKIFQRQSMKMSLSSCVVDA
Snf2 1178 VIIFDTDWNPHQDLQAQDRAHRIGQKNEVRILRLITTNSVEEVILERAYKKLDIDGKVIQA
XP_011393939_Nc 1746 VIFVEHDWNPQKDLQAMDRAHRIGQKKVVNVYRLITRGTLEEKIISLQRFKIDVASTVVNQ
XP_013950971_Tv 965 VIIYDSDWNPHQDLQAQDRAHRIGQKNEVRILRLISSNSVEEKILERARFKLDMDGKVIQA
XP_013951860_Tv 798 IIIFDPDWNPSTDLQARERAWRLGQNKPVKIYRLMTEGTIEEKIYHRQIFKQFMTNKVLKD
XP_013954753_Tv 1059 VFMMDPWWSYAVELQAIDRVHRLGQQDEVVVKRFIVRGSVEERMLKIQERKKFIATSLGMM
XP_013957450_Tv 651 LVLFDPDWNPAADQQALARVWRDGQTKDCFVYRFIATGTIEEKIFQRQSHKQSLSSCVVDS
XP_013958788_Tv 1586 VIFVEHDWNPQKDLQAMDRAHRIGQKKVVNVYRLITRGTLEEKIISLQRFKIDVASTVVNQ
XP_013960202_Tv 885 VFIVDPWWNPAAEWQSADRCHRIGQQRPCVITRLCIEDSVESRMVLIQEKKTSMIHSTVNA
XP_013960510_Tv 614 AYLMEPHWNPTLEDQALARIHRIGQTKEVTTIRFIVRDSEEERVVELQKSKTDLAEVIHRQ
XP_957128_Nc 946 VIIYDSDWNPHQDLQAQDRAHRIGQKNEVRILRLISSASVEEKILERARFKLDMDGKVIQA
XP_958511_Nc 1148 VYMMDPWWSFAVEAQAIDRVHRMGQEDPVRVYRFIVKQSVEMRMLRVQERKKFIATSLGMM
XP_959470_Nc 663 LVLFDPDWNPAADQQALARVWRDGQKKDCFVYRFIATGTIEEKIFQRQSHKQSLSSCVVDS
XP_961377_Nc 999 VFIVDPWWNPAAEWQSADRCHRIGQSRPCTITRLCIEDSVESRMVLLQEKKTNMINSTINA
XP_962958_Nc 822 VIIFDPDWNPSTDVQARERAWRLGQKKEVTIYRLMTAGTIEEKIYHRQIFKQFLSNKVLKD

Supplementary Fig. S4. Multiple sequence alignment of IPA-1 with proteins of the SNF2 family. Multiple sequence alignment of IPA-1 with members of the subfamilies of the SNF2 family of chromatin remodelers/helicase family-related proteins from *S. cerevisiae*, including Rad16, Mot1, Rad54, Rad5, Rad16, Uls1, Fun30, Chd1, Snf2, Irc5, Swr1, Ino80 and Isw2 and their relatives from *Neurospora crassa* and *T. virens*. Identical amino acids are highlighted in black, whereas conservative replacements are highlighted in gray. Tv, *T. virens*; Nc, *N. crassa*

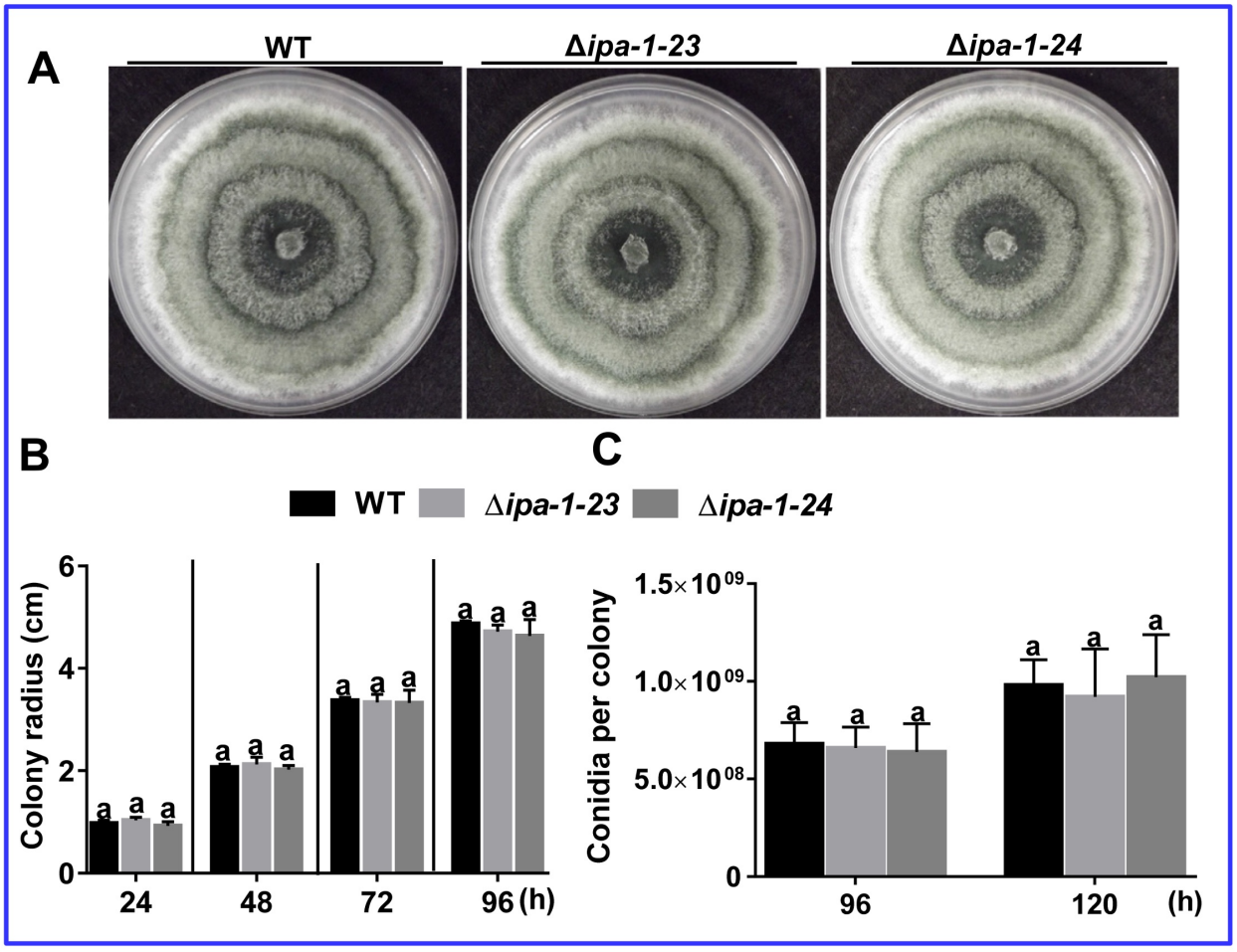

Supplementary Fig. S5. *T. virens* deletion mutants in *ipa-1* are not affected in growth or conidiation. A, Representatives photographs showing the growth of the WT, Δ*ipa-1-23* and Δ*ipa-1*-24 after 72h of growing on PDA. **B**, Colony radius of the WT, Δ*ipa-1-23* and Δ*ipa-1*-24 at 24, 48, 72 and 96 h of growing on PDA. **C**, Production of conidia of WT, Δ*ipa-1-23* and Δ*ipa-1*-24 strains after 96 and 120 h of growing on PDA. Data from (B-C) show the mean ± SD of three independent experiments, with at least 3 plates per condition. Results were validated with an analysis of variance statistical analysis with a Tukey multiple comparison test ($\alpha = 0.05$), different letters represent means statistically different at the 0.05 level.

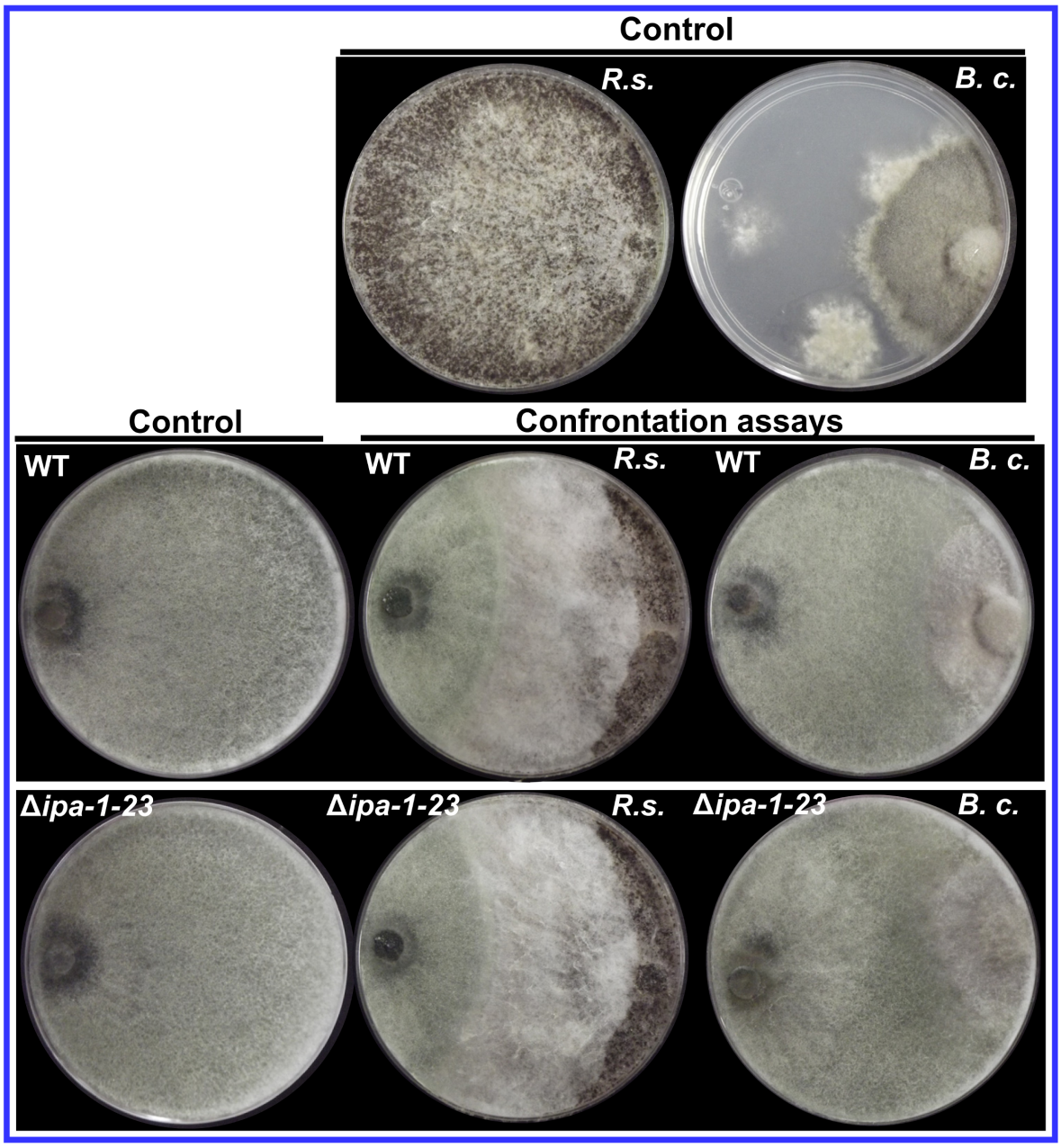

Supplementary Fig. S6. The absence of *ipa-1* did not impair the ability of *T. virens* to grow over the phytopathogens *R. solani* and *B. cinerea.* Confrontations assays were carried out by 7 days at 28 °C in darkness. Representative photographs of dual confrontation plates with the WT and Δ*ipa-1-23* (always left) against *R. solani* and *B. cinerea* plant-pathogens (always right). The dual confrontation was repeated thrice with similar results.

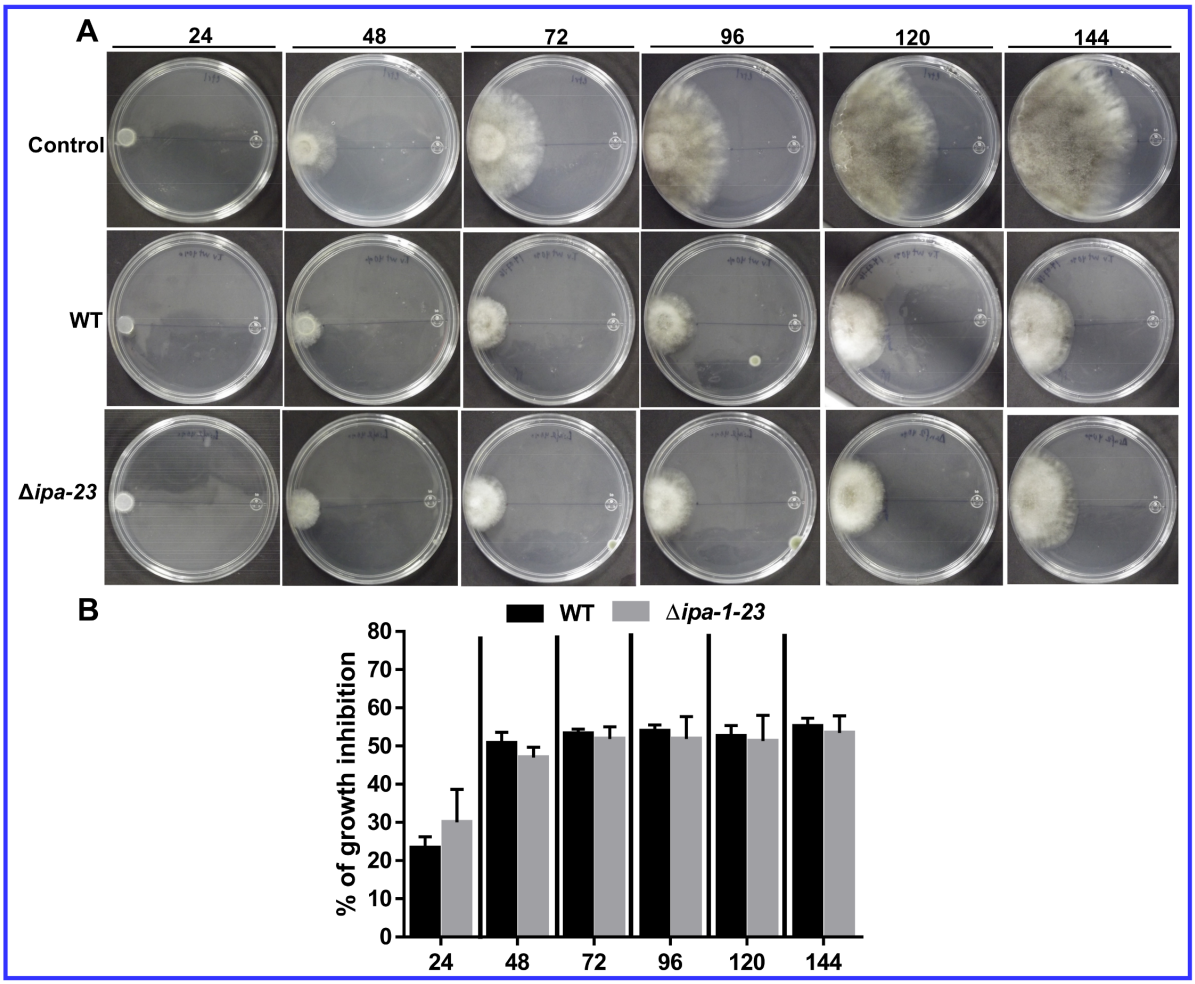

Supplementary Fig. S7. Mycelial free culture Filtrates (MFCF) of Δ*ipa-1-23* did not affect *B. cinerea* radial growth. The WT and Δ*ipa-1-23* strains were grown in PDB media for 4 days and MFCF were used to prepare PDA plates at 40%. **A**, Representative pictures of *B. cinerea* radial growth at 24, 48, 72, 96, 120 and 144h of culture on MFCF. **B,** Percentage of *B. cinerea* growth inhibition at 24, 48, 72, 96, 120 and 144h of culture on PDA plates containing MFCF. Data from (B) show the mean ± SD of three independent experiments (3 plates for treatment). Results were validated with an analysis of variance statistical analysis with a Tukey multiple comparison test (α= 0. 05), different letters represent means statistically different at the 0.05 level.

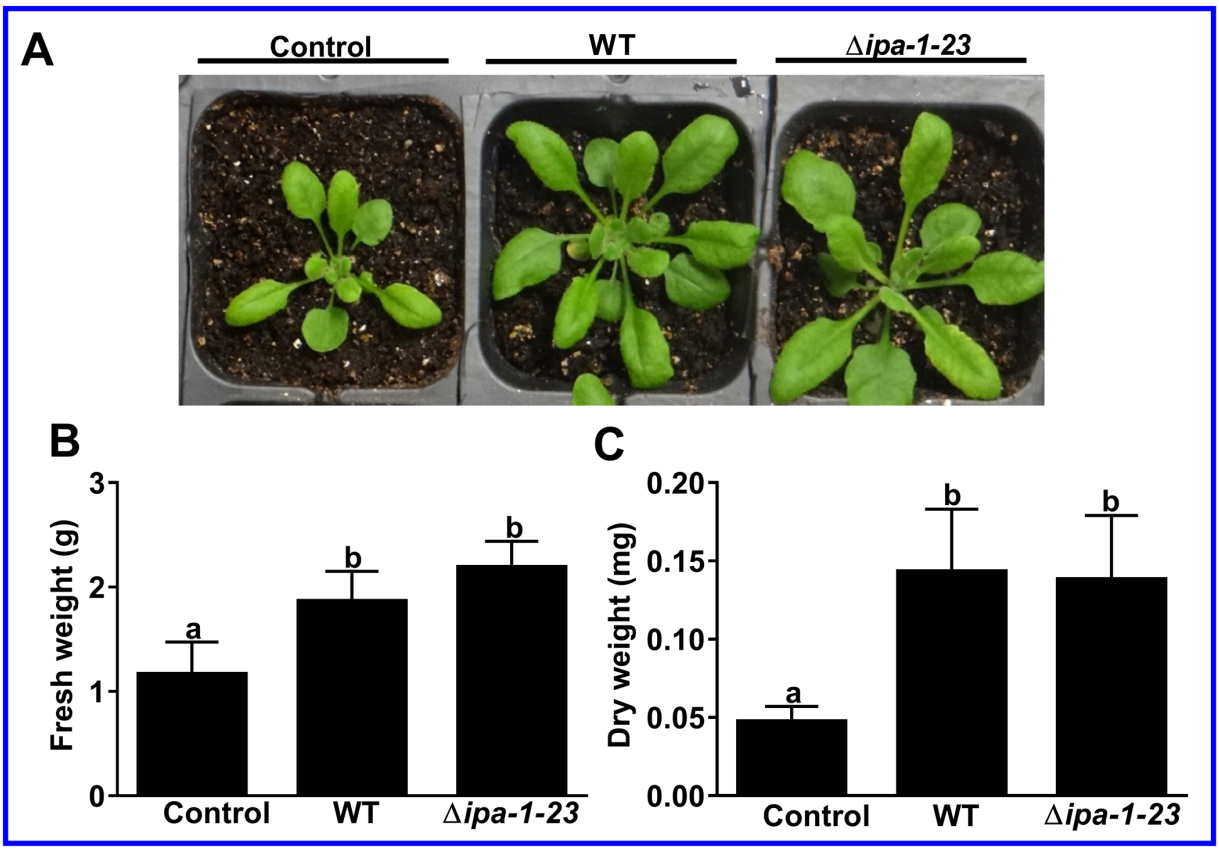

Supplementary Fig. S8. Deletion of *ipa-1* did not affect the plant growth-promoting activity of *T. virens*. Ten-day-old Arabidopsis seedlings grown on MS medium, and co-incubated for 14 days with the WT or Δ*ipa-1-23*. **A**, Representative picture of Arabidopsis grown under the indicated treatments. **B**, Fresh weight. **C**, Dry weight. Data from (B-C) shows the mean ± SD of two independent experiments (30 plants for each treatment). Results were validated with an analysis of variance statistical analysis with a Tukey multiple comparison test (α= 0. 05), different letters represent means statistically different at the 0.05 level.

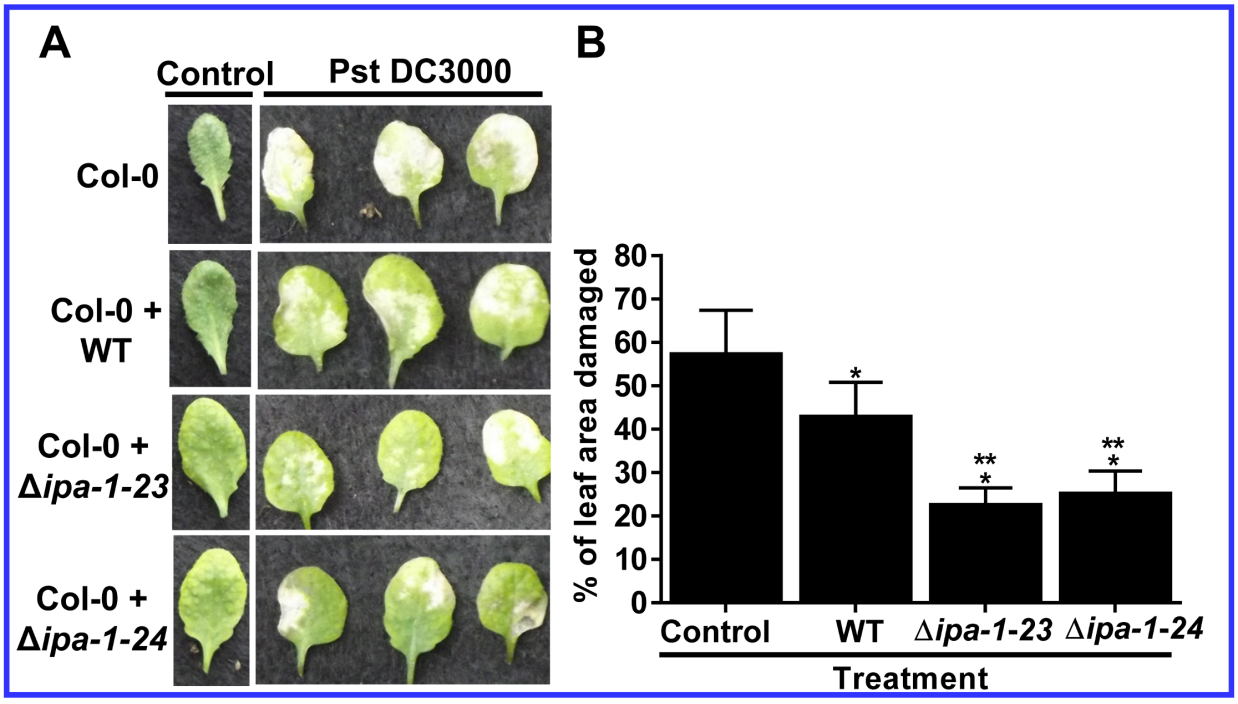

Supplementary Fig. S9. Deletion of *ipa-1* resulted in an enhanced plant protection against *P. syringae*. A, Representative images of leaves from 10-day-old Arabidopsis grown in soil and inoculated with the WT, Δ*ipa-1-23* or Δ*ipa-1*-24, and two weeks later infected with *Pst* DC3000 or inoculating buffer as control. **B**, Lesion sizes of infected plants with *Pst* DC3000 were determined using ImageJ**.** Data from (B) show the mean ± SD of at least 9 leaves. Asterisks indicate significant difference (independent Student's t-test, $P < 0.05$). *significant difference between Control vs. WT, Δ*ipa-1-23* or Δ*ipa-1*-24. **significant difference between WT vs. Δ*ipa-1-23* or Δ*ipa-1*-24.

Supplementary Table S1. Primers used for RNA-Seq Validation by RT-qPCR

Primer Name/Id	Primer Forward (5'-3')	Primer Reverse (5'-3')
EF-1-300828	CAGGTCGGTGCCGGATAC	TCAGAGAACTTGCAGGCAATGT
SM1	CCATCTACGTCTTGGCTGTTGA	GCATCGAGCGCAATGTTG
TBRG-1-70852	TGCCAATGTGGCGAGTATCA	CGTGGCTGGCTAGTTGACACT
SET-77874	GAATGGCGGCCTTGGATT	TCCACTCAGTTCTCGTGACGTT
GT4-83336	AGTTGCACGAGCGAATGTCA	TCCAACTTCGCACGAAACAC
GH18-194859	TGAACTTTCTGGGCATTGCA	CGCTCCCCCTTCTGATAGC
GST-2-227149	GCTCTGCTTGAGGCTGGACTT	GTCACGCTCCCAATTTGGA
NOX-69153	CCCTCGTCTCGCCTCTAGTCT	CGCTGCACACTCGTCAAGA
RTA1-59885	CTGGATGCACTGCCAATGTT	TCGCCAGGGTATTTCCAATG
AQP-6760	GATGGCGGGAAGCTGGAT	CCCAAAAGACGACGCAATGT
PFP-1-46295	GGCCGAACCCACTCACTTT	CATGGCGACGGATGAACTC
GST-1- 34822	AAGCAATCACCCCGTTGGT	CCAAAACATCGGGAGAATGAA
OXRDTASE-57247	CCAGGAGAGCCGCTGCTA	TGGCCGTTTCCGTCGAT
3HCD-46955	CGC CTG GAG CTC ACG AA	TTGTCACCCACTCGTGTTTCA
HSP-23-215292	GCACGAGTCGGGCTTTGA	CCTTGTTCTCGGGCTTCTTCT
SLAC-1-158830	TTGCCCGTTGCACCTCTAG	AGACTTTTCCCAGCTGCATGA
TvHyd1-143417	CAAGGCCCCGAGGTTGA	TCCCCCAGAGAAGGAATGC
PFP-2-69268	TCATGGAAGCCGTAAAAACGT	GCCTTTGCCACGGTTGAGT
GH7-90504	CGATTGCCCCCATCCA	TTGCCCGTAGTGCGTTTGA
KIN-58043	GCCCAAGCCGATAAGAAAGG	ATTATTCCGTATTTGCGCCATT
IPA-1-113458	GCCGTGGGATTAGCAGCAT	GGCGAAAGGGCAGAAAGTCT

Supplementary Table S2. Primers used for *ipa-1* deletion, *ipa-1* replacement confirmation, and determination of *ipa-1* copy number

***ipa-1* deletion**	
Primer Name	**Primers (*5'-3'*)**
5'SNF2-F	TCTCTCATATCTTTTGACTCGGATAGG
5' SNF2-R-Fusion	CTCCTTCAATATCAGTTAACGTCGATC ATCCCATGAAATGACAAACTCCATTTA
3 SNF2-F-Fusion	GCGCACTCGTCCGAGGGCAAAGGAATAG CTAGAGGTTCGTATAACAGTATCATGGC
3 SNF2-R	CTTGAAGAACGCTGGATATAGGGTC
DJhph-F	GATCGACGTTAACTGATATTGAAGGA
DJhph-R	CTATTCCTTTGCCCTCGGACGAGTGC
***ipa-1* gene replacement confirmation**	
5'SNF2-F'-Upstream	TTTTGCCGCTCCCAACGCAGC
3'SNF2-R'-Downstream	ACTTGGATCGAGGCAAGGCAG
Id-Mut R	ACAGCGGGCAGTTCGGTTTCA
Id-Mut F	ATAGTGGAAACCGACGCCCC
***ipa-1* and *hph* gene copy number determination**	
SNF2-TR-F	GCCGTGGGATTAGCAGCAT
SNF2-TR-R	GGCGAAAGGGCAGAAAGTCT
HPH-TR-F	CCTCGTGCATGCGGATTT
HPH-TR-R	GCTGTTATGCGGCCATTGT

Supplementary Table S3. Primers used to analyze defense responsive genes in *A. thaliana*

Primer Name/ TAIR Locus	**Primer Forward (5'-3')**	**Primer Reverse (5'-3')**
ACTIN 2/AT3G18780	TGTGACAATGGTACCGGTATG	CAGCCCTGGGAGCATCAT
PR-1a/AT2G14610	ATCTAAGGGTTCACAACCAGGCAC	TGCCTCTTAGTTGTTCTGCGTAGC
PDF1.2/ AT5G44420	CACCCTTATCTTCGCTGCTC	GGAAGACATAGTTGCATGATCC

Supplementary Table S4. List of differentially expressed genes of *T. virens* during interaction with *A. thaliana* at 48, 72 and 96 h post inoculation (TvAt vs Tv, FDR<0.05, and log2FC >1). The cluster number to which genes belong is shown according to hierarchical clustering.

Supplementary Table S5. List of GO terms enriched in the differentially expressed genes during *T. virens-A. thaliana* interaction at 48 hours post inoculation (FDR<0.05).

Supplementary Table S6. Relative expression of 19 differentially expressed genes, grouped at different clusters at 48, 72 and 96 of co-culture by RNA-Seq.

	Fold change		
Cluster 1	**48 h**	**72 h**	**96 h**
1. hypothetical Serine/threonine protein kinase, TRIVIDRAFT_58043	0.18		
2. small heat shock protein -23, TRIVIDRAFT_215292	0.04		4.50
Cluster 2			
3. Glycoside Hydrolase Family 18 protein, TRIVIDRAFT_194859	0.00		
4. Glycoside hydrolase family 7, TRIVIDRAFT_90504	0.00	0.00	0.00
5. Glycosyltransferase family 4 protein, TRIVIDRAFT_83336	0.01		
Cluster 4			
6. hypothetical Oxidoreductase NAD-binding domain, TRIVIDRAFT_57247	0.19	4.96	
7. hypothetical Glutathione-S-transferase -2, TRIVIDRAFT_227149		117.78	
8. hypothetical Aquaporin, TRIVIDRAFT_6760			0.24
Cluster 6			
9. hypothetical 3-hydroxyacyl-CoA dehydrogenase, TRIVIDRAFT_46955	18.56	4.40	
10. hypothetical lysine methyltransferase [HMKT]-TRIVIDRAFT_77874	7.85		
11. hypothetical chromatin remodeler- *ipa-1,* TRIVIDRAFT_113458	4.45		
12. hypothetical Big Ras GTPase -1 *tbrg-1*, TRIVIDRAFT_70852	20.96		
Cluster 7			
13. hypothetical Glutathione-S-transferase, TRIVIDRAFT_34822	7.56	10.81	5.30
14. hypothetical Glutamine amidotransferase -1, TRIVIDRAFT_46295	3.78	45.74	7.74
15. hypothetical hydrophobin TvHyd1, TRIVIDRAFT_143417		7.00	2.94
16. hypothetical Glutamine amidotransferase -2, TRIVIDRAFT_69268		41.45	11.06
17. hypothetical unknown uptake transporter, TRIVIDRAFT_158830		11.32	18.27
18. hypothetical Ferric reductase-like transmembrane component, TRIVIDRAFT_69153			11.36
19. hypothetical-binding protein to unknown toxic compounds, TRIVIDRAFT_59885			8.59

Supplementary Table S7. Copy numbers of the *ipa-1* and *hph* genes determined by the $2^{-\Delta\Delta Ct}$ method

Strain	Ct of endogenous control (Ct_e)	Ct of transgene (Ct_t)	ΔCt (Ct_t-Ct_e)	ΔΔCt (ΔCt_s-ΔCt_c)	Copy number (2^-ΔΔCt)
	tef-1	***ipa-1***			
Δ*sm-1*	22.90	14.72	-8.18	0.00	1.00 ± 0.00
Δ*ipa-1-23*	22.19	25.42	3.22	11.40	0.00 ± 0.00
Δ*ipa-1-24*	22.17	28.51	6.34	14.52	0.00 ± 0.00

Strain	Ct of endogenous control (Ct_e)	Ct of transgene (Ct_t)	ΔCt (Ct_t-Ct_e)	ΔΔCt (ΔCt_s-ΔCt_c)	Copy number (2^-ΔΔCt)
	tef-1	***hph***			
Δ*sm-1*	22.90	18.97	-3.93	0.00	1.00 ± 0.00
Δ*ipa-1-23*	22.19	18.09	-4.11	-0.18	1.13 ± 0.08
Δ*ipa-1-24*	22.17	18.05	-4.12	-0.19	1.14 ± 0.06